New Cretaceous neosuchians (Crocodylomorpha) from Thailand bridge the evolutionary history of atoposaurids and paralligatorids

Yohan Pochat-Cottilloux, Komsorn Lauprasert, Phornphen Chanthasit, Sita Manitkoon, Jérôme Adrien, Joël Lachambre, Romain Amiot, Jeremy E Martin

Zoological Journal of the Linnean Society, 2023, **XX**, 1–27
https://doi.org/10.1093/zoolinnean/zlad195
Advance access publication XX XX XXXX
Original Article

OXFORD

AQ1-AQ4

Original Article

New Cretaceous neosuchians (Crocodylomorpha) from Thailand bridge the evolutionary history of atoposaurids and paralligatorids

Yohan Pochat-Cottilloux[1,*], Komsorn Lauprasert[2], Phornphen Chantasit[3], Sita Manitkoon[2], Jérôme Adrien[4], Joël Lachambre[4], Romain Amiot[1], Jeremy E. Martin[1]

AQ5

[1]Univ Lyon, Univ Lyon 1, ENSL, CNRS, LGL-TPE, Villeurbanne, France
[2]Palaeontological Research and Education Centre, Mahasarakham University, Maha Sarakham, Thailand
[3]Sirindhorn Museum, Department of Mineral Resources, Kalasin, Thailand
[4]Laboratoire Matériaux, Ingénierie et Science, Institut National des Sciences Appliquées de Lyon, Villeurbanne, France

[*]Corresponding author. Univ Lyon, Univ Lyon 1, ENSL, CNRS, LGL-TPE, Villeurbanne, France. E-mail: yohan.pochat@orange.fr

AQ6

ABSTRACT

AQ8

The origin of modern crocodylians is rooted in the Cretaceous, but their evolutionary history is obscure because the relationships of outgroups and transitional forms are poorly resolved. Here, we describe a new form, *Varanosuchus sakonnakhonensis* gen. nov., sp. nov., from the Early Cretaceous of Thailand that fills an evolutionary gap between Paralligatoridae and Atoposauridae, two derived neosuchian lineages with previously unsettled phylogenetic relationships. Three individuals, including a complete skull and associated postcranial remains, allow for a detailed description and phylogenetic analysis. The new taxon is distinguished from all other crocodylomorphs by an association of features, including a narrow oreinostral morphology, a dorsal part of the postorbital with an anterolaterally facing edge, a depression on the posterolateral surface of the maxilla, and fully pterygoid-bound choanae. A phylogenetic analysis confirms the monophyly and taxonomic content of Atoposauridae and Paralligatoridae, and we underline the difficulty in reaching a robust definition of Eusuchia. Furthermore, we put forward further arguments related to the putative terrestrial ecology with semi-aquatic affinities of atoposaurids based on their oreinostral snout morphology and osteoderm ornamentation.

Keywords: Crocodylomorpha; computed tomography; morphological comparison; skull anatomy; palaeoecology; semi-terrestrial; Asia; Cretaceous; endocasts; palaeontology

INTRODUCTION

Neosuchia are a crocodylomorph clade that appeared during the Jurassic and gave rise during the Cretaceous to modern forms (Salisbury *et al.* 2006). Although its major lineages, including Goniopholididae, Pholidosauridae, Dyrosauridae, Atoposauridae, Paralligatoridae, and Eusuchia, are generally considered monophyletic (Jouve *et al.* 2006, Turner 2015, Martin *et al.* 2016a, Tennant *et al.* 2016, Meunier 2017, Ristevski *et al.* 2018), their interrelationships are still heavily debated. One major problem of this situation is the poor resolution over the origin and evolutionary processes at the neosuchian–eusuchian transition. For example, although Eusuchia are classically diagnosed as possessing pterygoid-bound choanae, procoelous vertebral centra, and a sagittal segmentation of the paravertebral shield (Benton and Clark 1988, Clark 1994), this can no longer be considered the norm, and their evolutionary history is more complex than originally admitted (Salisbury *et al.* 2006, Turner and Buckley 2008, Pol *et al.* 2009, Sweetman *et al.* 2014, Turner 2015, Turner and Pritchard 2015, Tennant *et al.* 2016, Leite and Fortier 2018, Martin *et al.* 2020). Thus, those issues remain highly debated, particularly about the timing of the transition between 'basal' neosuchians and eusuchians, about which clade(s) are closer to Eusuchia, and about which characters support those changes.

Among the fossils of particular interest to these issues are those belonging to the families Atoposauridae and Paralligatoridae, both of which have been rediagnosed recently

Received 21 June 2023; revised 17 November 2023; accepted 30 November 2023
[Version of Record, published on XX XXX XXXX; http://zoobank.org/urn:lsid:zoobank.org:pub:XXXXX]

AQ7

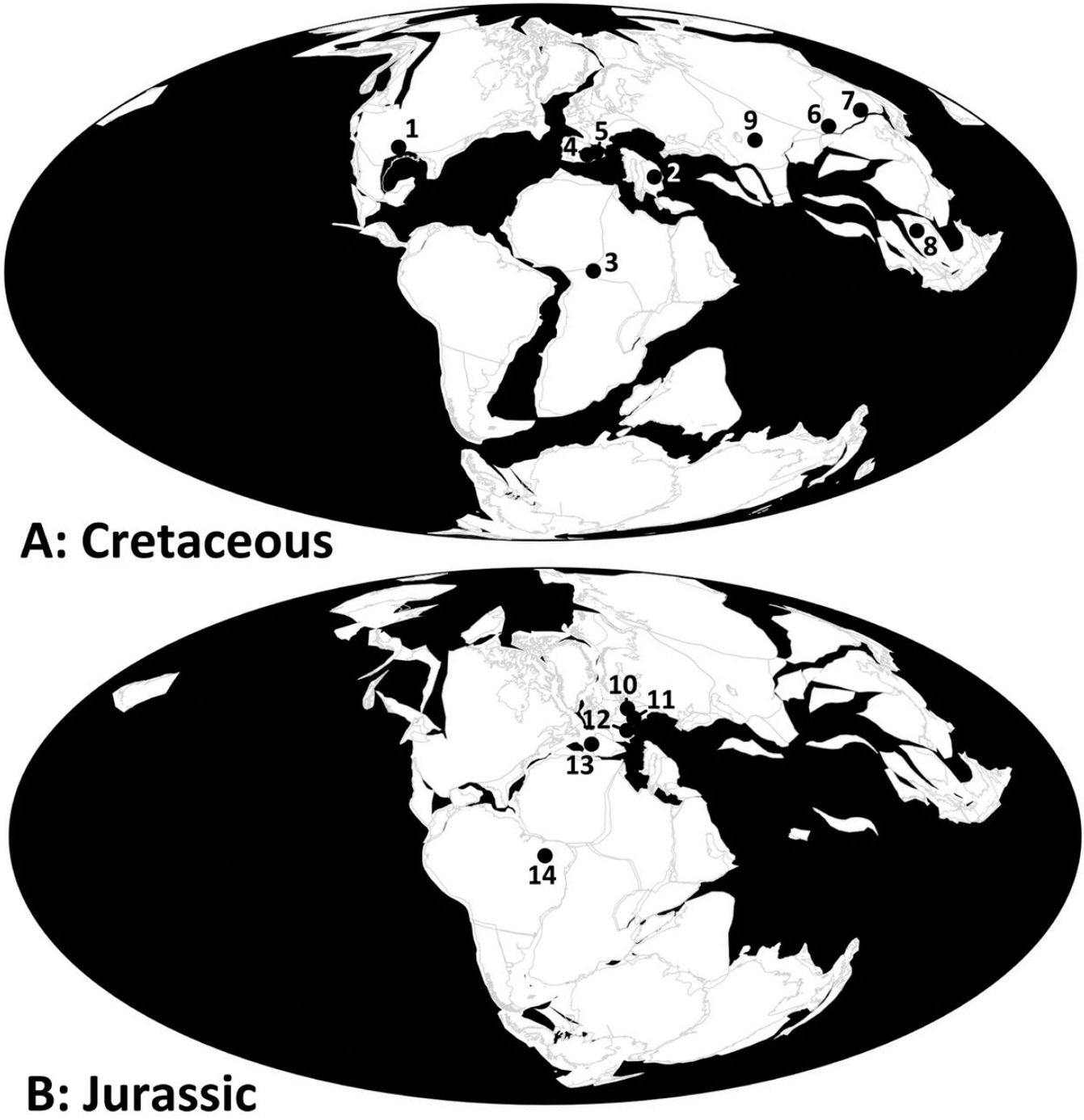

Figure 1. Palaeogeographical distribution of putative atoposaurid and paralligatorid taxa: 1, *Wannchampsus kirpachi*, *Tarsomordeo winkleri*, Glen Rose Form (Aptian, USA), and *Scolomastax sahlsteini* (Cenomanian, USA); 2, *Aprosuchus ghirai* and *Sabresuchus sympiestodon* (Maastrichtian, Romania); 3, *Brillanceausuchus babouriensis* (Barremian, Cameroon); 4, *Sabresuchus ibericus* (Barremian, Spain); 5, *Montsecosuchus deperiti* (Barremian, Spain); 6, *Shamosuchus djadochtaensis* and *Paralligator gradilifrons* (Cenomanian–Campanian, Mongolia); 7, *Rugosuchus nonganensis* (Campanian, China) and *Yangjisuchus longshanensis* (Albian–Cenomanian, China); 8, *Theriosuchus grandinaris* and Phu Sung specimens described here (Barremian, Thailand); 9, *Kansajsuchus extensus* (Santonian–Campanian, Kazakhstan–Tadzhikistan); 10, *Knoetschkesuchus langenbergensis* (Kimmeridgian, Germany); 11, *Alligatorellus* and *Atoposaurus oberndorferi* (Tithonian, Germany); 12, *Alligatorium* and *Atoposaurus jourdani* (Kimmeridgian, Germany); 13, *Knoetschkesuchus guimarotae* (Kimmeridgian, Spain); 14, *Batrachomimus pastosbonensis* (Oxfordian–Kimmeridgian, Brazil). Maps are from Paleobiology Database.

(Turner 2015, Tennant *et al.* 2016, Adams 2019, Kuzmin *et al.* 2019, Noto *et al.* 2020, Rummy *et al.* 2022). Atoposaurids *sensu* Tennant *et al.* (2016) comprise only five species from the Late Jurassic of France and Germany (Fig. 1; Tennant *et al.* 2016 and references therein), and paralligatorids *sensu* Rummy *et al.* (2022) comprise ≥11 taxa from the Late Jurassic to the Cretaceous, distributed worldwide (Fig. 1; Turner 2015, Tennant *et al.* 2016, Adams 2019, Kuzmin *et al.* 2019,

Noto *et al.* 2020, Rummy *et al.* 2022 and references therein). Given that those two families exhibit several variable morphological characters among those historically considered as autapomorphies of Eusuchia (see above), they are thus ideal candidates for illustrating the Neosuchia–Eusuchia transition. A better understanding of the relationships of those taxa is essential to understand the neosuchian diversification and palaeobiogeographical evolution through time. Virtually nothing is known about their ecology, although Schwarz and Salisbury (2005) and Martin *et al.* (2014) hypothesized a terrestrial ecology for atoposaurids based on their very scarce fossil record, given that terrestrial environments are less prone to good conservation conditions.

Here, we describe three new specimens belonging to a new species of atoposaurid from the Early Cretaceous Sao Khua Formation of Thailand (early Valanginian–early Hauterivian; Tucker *et al.* 2022). The specimens (Figs 2–15; Supporting Information, Supplementary Materials S1–S3; Supplementary Models S1–S7) come from the Phu Sung locality, a reddish micaceous silty mudstone continental deposit, and were found together within a faunal assemblage composed of sharks, bony fishes, and turtles (Chanthasit *et al.* 2019, Ditbanjong *et al.* 2019). Although another atoposaurid was previously known in the Cretaceous of Thailand (Lauprasert *et al.* 2011), they are of particular importance for proposing a new phylogenetic framework close to the Neosuchia–Eusuchia transition and highlight that Southeast Asia still holds an under-evaluated fossil record for understanding the evolution of neosuchians, and particularly of atoposaurids and paralligatorids.

MATERIALS AND METHODS

Character taxon matrix and coding

The character taxon matrix used in this paper consists of 80 operational taxonomic units and 321 multistate characters (Supporting Information, Supplementary Materials S4 and S5); the outgroup is *Gracilisuchus stipanicicorum* Romer, 1972; all characters involved in the parsimony analysis are equally weighted and unordered.

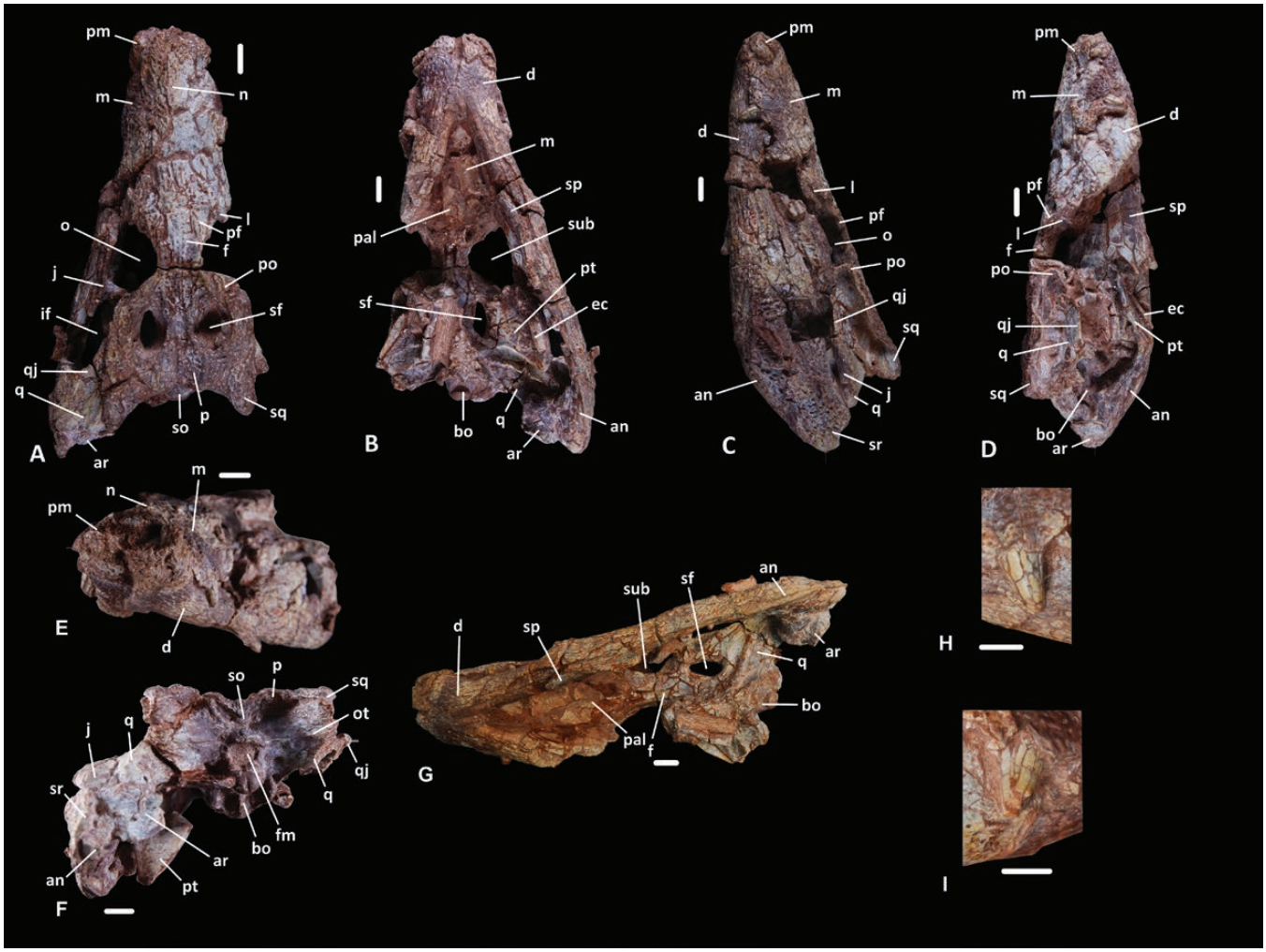

Figure 2. SM-2021-1-97: main part of the skull in dorsal (A), ventral (B), lateral (C, D), anterior (E), posterior (F), and lateroventral (G) views. H, I, two teeth visible in external view. Abbreviations: an, angular; ar, articular; bo, basioccipital; d, dentary; ec, ectopterygoid; f, frontal; fm, foramen magnum; if, infratemporal fenestra; j, jugal; l, lacrimal; m, maxillary; n, nasal; o, orbit; ot, otoccipital; p, parietal; pal, palatine; pf, prefrontal; pm, premaxillary; po, postorbital; pt, pterygoid; q, quadrate; qj, quadratojugal; sf, supratemporal fenestra; so, supraoccipital; sp, splenial; sq, squamosal; sr, surangular; sub, suborbital fenestra. Scale bars: 1 cm.

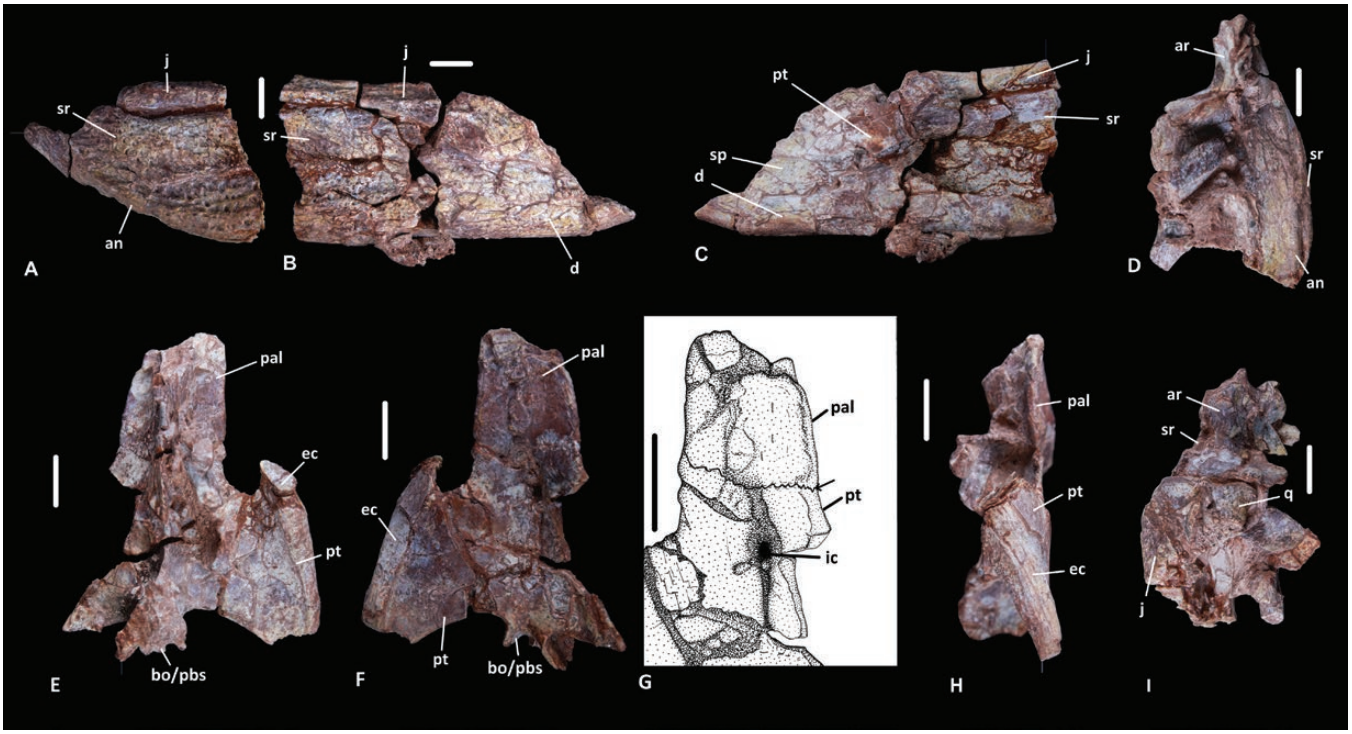

Figure 3. SM-2021-1-97: mandibular and pterygoid parts of the skull in lateral (A, B, H), medial (C), dorsal (E, I), and ventral (D, F, G) views. Abbreviations: an, angular; ar, articular; bo, basioccipital; d, dentary; ic, internal choana; j, jugal; pal, palatine; pbs, parabasisphenoid; pt, pterygoid; q, quadrate; sp, splenial; sr, surangular. Arrow in G indicates palatine–pterygoid suture. Scale bars: 1 cm.

This character taxon matrix, to which we added the scorable osteological characters of the specimens described here, is taken from the complete dataset of Schwarz *et al.* (2017), modified from Turner (2015), with some adjustments made by Venczel and Codrea (2019). *Knoetschkesuchus guimarotae* Schwarz & Salisbury, 2005 scorings were updated following Eijkelboom (2020), and *Shamosuchus ulanicus* Efimov, 1983 was removed because it is a junior synonym of *Paralligator gradilifrons* Konzhukova, 1954, which now regroups *Shamosuchus ancestralis sensu* Konzhukova (1954), *Shamosuchus ulgicus sensu* Efimov (1981), *Shamosuchus ulanicus sensu* Efimov (1983), and *Shamosuchus tarsus sensu* Efimov (1983) (Turner 2015). *Brillanceausuchus babouriensis* Michard *et al.*, 1990 and *Montsecosuchus deperiti* Vidal, 1915 were also not included, pending future reassessment of those taxa (Tennant *et al.* 2016). Although previously recovered nested within neosuchians, we also chose to remove thalattosuchians because they most probably branch basally or sister to Mesoeucrocodylia (Wilberg *et al.* 2022) and because the present study focuses on derived neosuchians. *Pachycheilosuchus trinquei* Rogers, 2003, *Tarsomordeo winkleri* Adams, 2019, *Scolomastax salhsteini* Noto *et al.*, 2020, and *Yanjisuchus longshanensis* Rummy *et al.*, 2022 were not added into the matrix because they are too incomplete; however, we added *Kansajsuchus extensus* Efimov, 1975 (Kuzmin *et al.* 2019) and *Theriosuchus grandinaris* Lauprasert *et al.*, 2011. Finally, some scorings were updated, and those of *Bernissartia fagesii* Dollo, 1883 were thoroughly revised on 80 characters, based on Martin *et al.* (2020) (see also Supporting Information, Supplementary Material S6). Only the two most complete specimens from Phu Sung (*SM-2021-1-97/101* and SM-2023-1-16) were scored, because the third one is too incomplete to warrant a robust phylogenetic assessment.

Phylogenetic analyses

The analyses were made in parsimony, on TNT v.1.5 (Goloboff and Catalano 2016). New Technology Search was used, enabling all search algorithms (Sectorial Search, Ratchet, Drift and Tree Fusing; Goloboff 1999, Nixon 1999). The default settings for these advanced search methods were changed only to increase the iterations of each method; it now features 100 sectorial search drifting cycles, 100 ratchet iterations, 100 drift cycles, and 100 rounds of tree fusion per replicate. This tree-space search procedure was repeated for 10 different random start seeds (following the procedure described by Jouve 2016) using a driven search to find the minimum length 10 times. Otherwise, the default parameters were retained. Extended implied weighting (Goloboff 2014) was not used because its utility remains controversial (Congreve and Lamsdell 2016, Groh *et al.* 2020). Bootstrap scores were then calculated. This procedure was validated further by a heuristic search of Wagner trees with 1000 random addition sequences, followed by tree bisection–reconnection and saving 10 cladograms per round (random seeds: 100). When necessary, the ACCTRAN optimization was used (accelerated transformation; Farris 1970, Swofford and Maddison 1987). FigTree v.1.4.4 was used to visualize the phylogenetic trees obtained.

Computed tomography scan

The CT scan was performed in January 2021 at the Laboratoire Mateis (INSA Lyon, Villeurbanne, France) on a DTHE (Double Tomographe Haute Energie by RX Solutions). Detailed acquisition parameters are available in the Supporting Information (Supplementary Material S7).

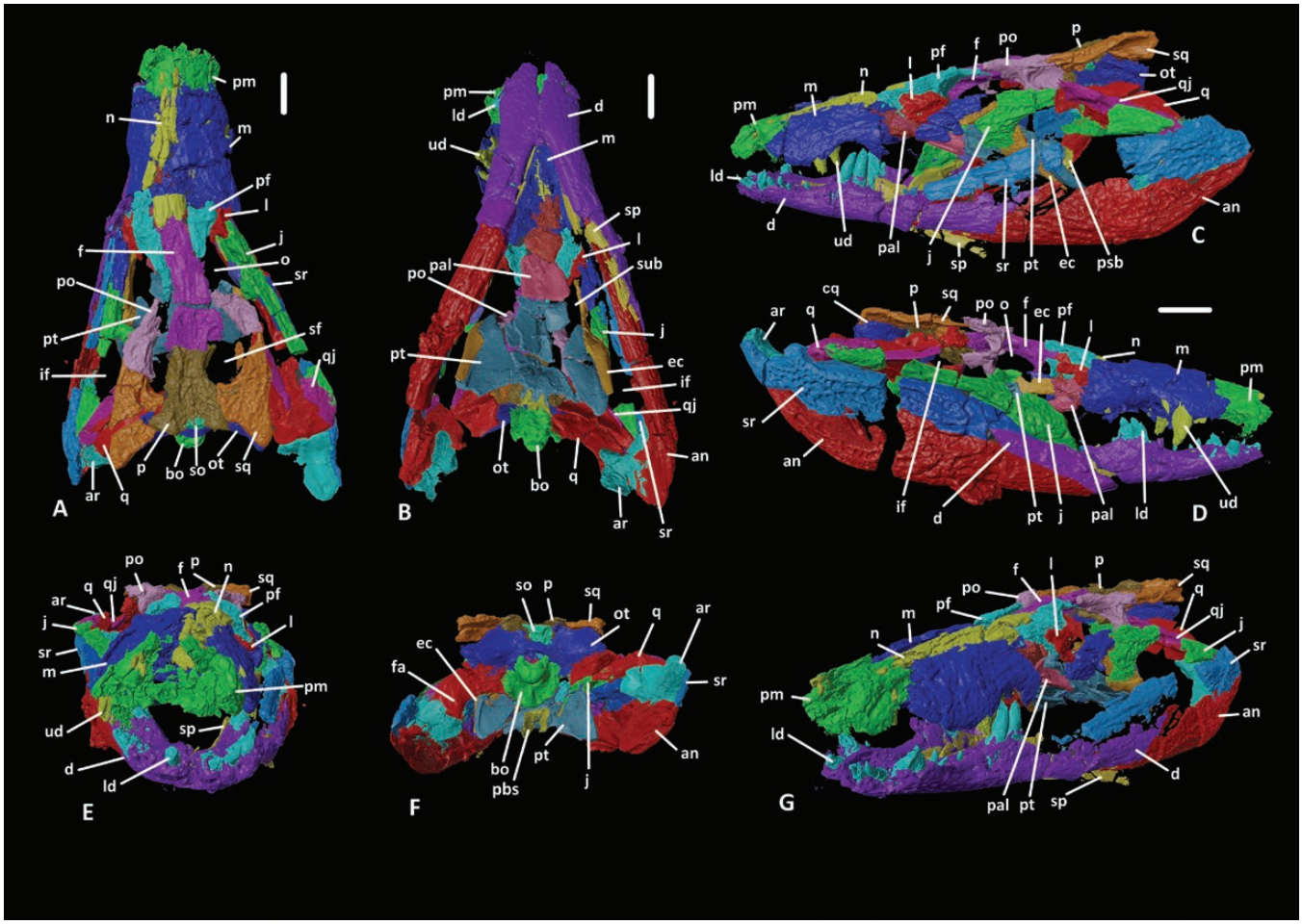

Figure 4. Three-dimensional reconstruction of SM-2021-1-97: full skull in dorsal (A), ventral (B), lateral (C, D), anterior (E), posterior (F), and anterior three-quarter (G) views. Abbreviations: an, angular; ar, articular; cq, cranioquadrate passage; d, dentary; ec, ectopterygoid; f, frontal; fa, foramen aërum; if, infratemporal fenestra; j, jugal; l, lacrimal; ld, lower dentition; m, maxillary; n, nasal; o, orbit; ot, otoccipital; p, parietal; pal, palatine; pbs, parabasisphenoid; pf, prefrontal; pm, premaxillary; po, postorbital; pt, pterygoid; q, quadrate; qj, quadratojugal; sf, supratemporal fenestra; so, supraoccipital; sp, splenial; sq, squamosal; sr, surangular; sub, suborbital fenestra; ud, upper dentition. Scale bars: 2 cm.

Institutional abbreviations

AR, Ariño collection, housed at Museo Aragonés de Paleontología, Teruel, Spain; DMR, Direction of Mineral Resources, Bangkok, Thailand; SM, Sirindhorn Museum, Kalasin, Thailand; USNM, Smithsonian National Museum of Natural History, Washington, DC, USA.

RESULTS

SYSTEMATIC PALAEONTOLOGY

Crocodylomorpha Hay, 1930

Mesoeucrocodylia Whestone and Whybrow, 1983

Neosuchia Clark, 1986

Atoposauridae Gervais, 1871

Varanosuchus gen. nov.

Type species: Varanosuchus sakonnakhonensis.

Derivation of name: Owing to its superficial resemblance to a monitor lizard.

Diagnosis: As for the type and only known species.

Varanosuchus sakonnakhonensis gen. nov., sp. nov.

Derivation of name: After the province of Sakon Nakhon, Thailand, where the holotype and referred specimens were found.

Holotype: SM-2021-1-97/101, a three-dimensionally preserved, almost complete skull, lacking its anteriormost part (anterior part of premaxilla and nasal), with associated mostly complete postcranial skeleton, involving the axial column and osteoderms. The specimen lacks most of the pectoral girdle (except for the coracoid) and all the forelimb elements. The pubis, tibia, fibula, and digit are the only elements known from the pelvic girdle and the hindlimbs.

Type locality: Phu Sung locality, near Mueang Nakhon, Sakon Nakhon district, Thailand.

Stratigraphic horizon and range: The geological strata from which the new taxon originates belong to the Early Cretaceous Sao Khua Formation (Khorat Group) of Thailand (Chanthasit *et al.* 2019, Ditbanjong *et al.* 2019).

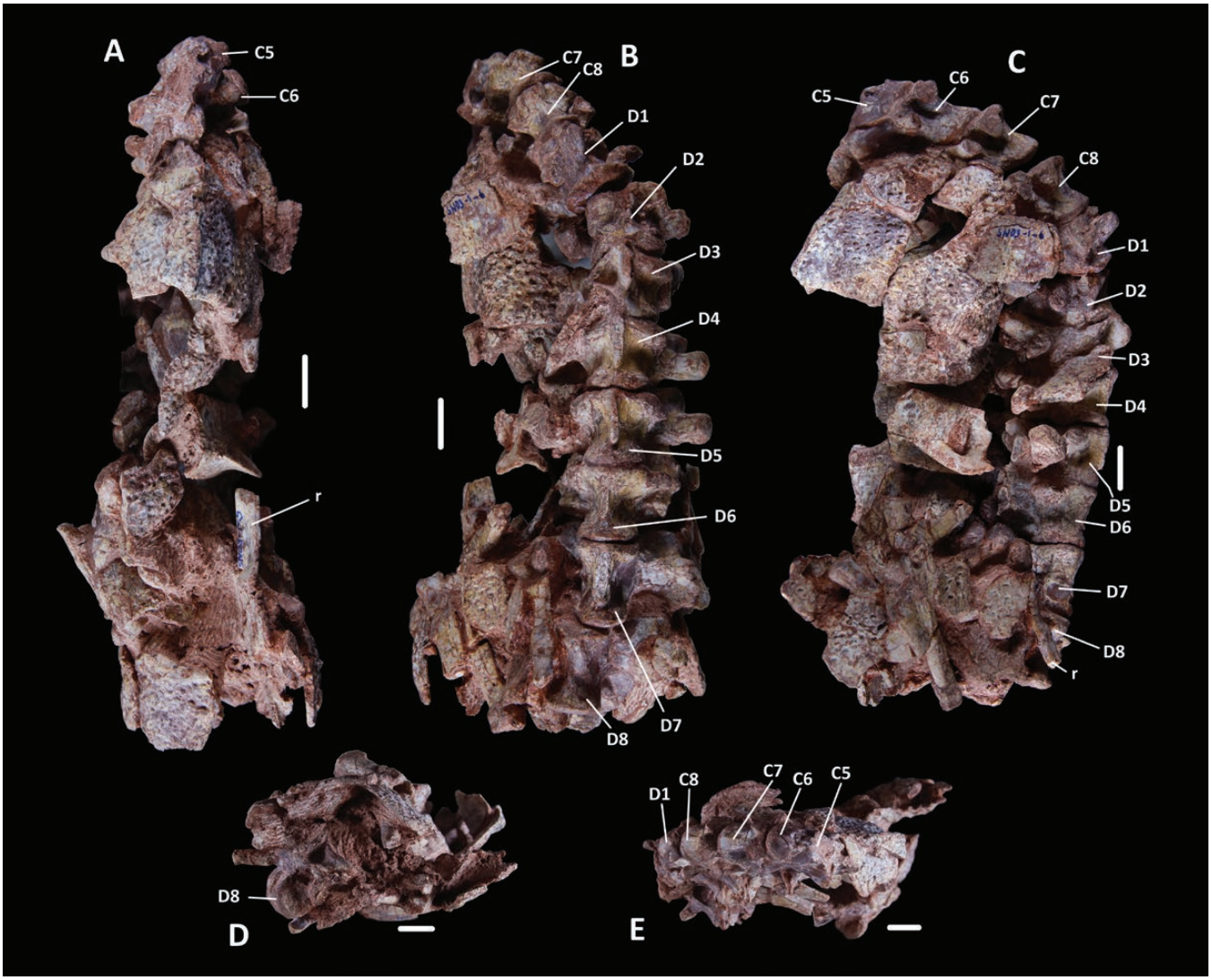

Figure 5. SM-2021-1-98: cervical vertebrae and osteoderms in dorsal (A), ventral (B), lateral (C), posterior (D), and anterior (E) views. Abbreviations: C5–C8, cervical vertebrae 5–8; D1–D8: dorsal vertebrae 1–8. Scale bars: 1 cm.

Referred specimens: SM-2023-1-16, a three-dimensionally preserved nearly complete skull. SM-2023-1-17, a three-dimensionally preserved partial skull table. Both specimens were found in the same strata as the holotype.

Diagnosis: a crocodylomorph characterized by the following unique combination of features: the dorsal part of the postorbital has an anterolaterally facing edge; the quadrate has no fenestrae; there are two waves of enlarged maxillary teeth; the quadratojugal has no ornamentation; the outer surface of the squamosal is laterodorsally oriented, reduced, and sculpted; and there is a depression on the posterolateral surface of the maxilla.

Description

Cranial openings

The sutures between the parietal, the supraoccipital and the otoccipital are thin anteroposteriorly, but there is no clear opening in this region (i.e. no 'true' posttemporal fenestrae). The internal choana is contained by the pterygoids (and maybe the palatines in SM-2023-1-16) and is situated immediately anterior to the contact with the palatine, anteriorly. No septum can be seen. The orbit is large, about half the length of the skull table. It is D-shaped in dorsal and lateral views. This opening is surrounded by the jugal, the maxilla, the lacrimal, the frontal, the prefrontal, and the postorbital. The margins are not upturned.

As in all diapsids, the skull possesses two pairs of temporal fenestrae: the supratemporal and infratemporal ones. The supratemporal fenestra is ovoid, with its longest axis directed anteroposteriorly and almost the same length as the parietal. The supratemporal fossa has steep vertical walls in SM-2021-1-97/99. The frontoparietal fossa is not apparent in *SM-2021-1-97/101* (owing to vertical walls) and not very wide, quickly disappearing ventrally in SM-2023-1-16 and SM-2023-1-17. The infratemporal fenestra is preserved on the left side in all specimens: it is not complete but appears triangular; it is bordered by the jugal laterally, the postorbital anteriorly, and the quadratojugal posteromedially. No spike-like projection inside the fenestra can be seen. In SM-2023-1-16, the antorbital fenestra is present near the triple junction between the maxilla, the lacrimal, and the jugal in lateral view (Figs 11D, 13D).

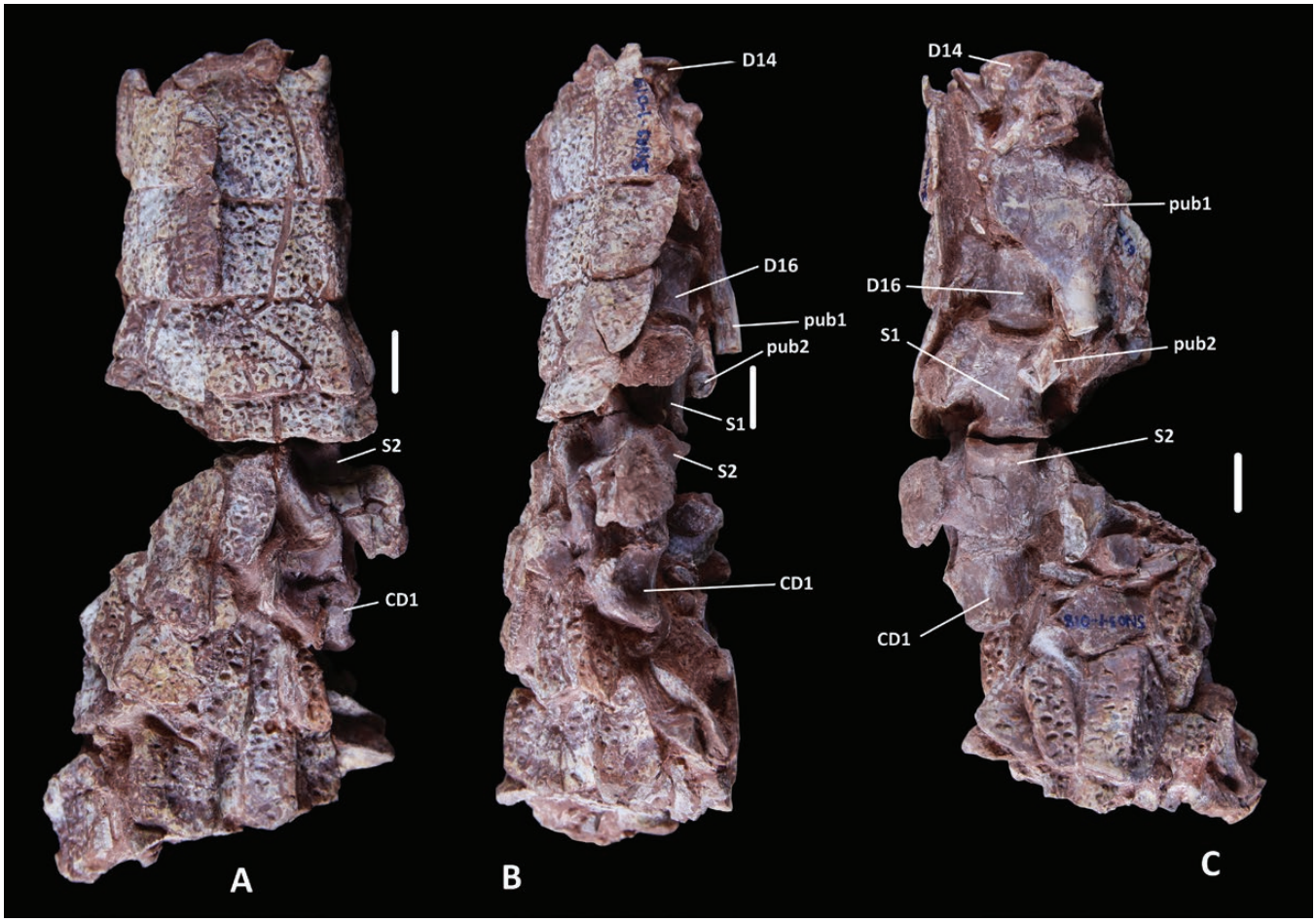

Figure 6. SM-2021-1-100: dorsal, sacral, and caudal vertebrae in dorsal (A), lateral (B), and ventral (C) views. Abbreviations: CD1, caudal vertebra 1; D14 and D16, dorsal vertebrae 14 and 16; pub1 and pub2, pubis 1 and 2; S1 and S2: sacral vertebrae 1 and 2. Scale bars: 1 cm.

The cranioquadrate canal appears open as a groove in lateral view, immediately ventral to the squamosal and posterior to the tympanic region. It is formed solely of the otoccipital in *SM-2021-1-97/101* and probably also in SM-2023-1-16, although it is difficult to assess because of the poor state of preservation.

The foramen magnum is triangular in shape and ~1 cm at its widest part.

Cranium (Figs 2–4,11–14)

The specimens are rather short-snouted; as a result, the rostrum makes up about half the size of the whole skull. The nasal is long, reaching the anterior limit of the skull. The braincase occupies the posterior one-third of the skull. The cranial table is ornamented with circular ovoid pits dorsally.

Premaxilla (Figs 2A, C–E, 4A–E, G, 11A–E, G, 12A, 13A–D): The premaxilla, together with the anterior part of the nasal, forms the anterior part of the snout. It is straight posteriorly, forming an oblique suture with the maxilla in lateral view. In dorsal view, the opening for the nares is mostly composed of the premaxilla, with participation by the nasal in its posterior part. On the ventral surface, the foramen incisivum is a single opening; it is unique and completely enclosed by the premaxillae. Although it is damaged, this opening is cylindrical, with the longest axis directed anteroposteriorly, but it does not abut the premaxillary toothrow (Supporting Information, Supplementary Model S3). The contact between the two bones is straight anteroposteriorly. The contact between the maxilla and the premaxilla is straight lateromedially in ventral view, oblique in lateral view, and straight lateromedially in dorsal view, with two posteriorly projecting processes of the premaxilla in SM-2021-1-97: one in the maxilla and one medially at the contact with the nasal. Medially in dorsal view and posterior to the nares, the two premaxillae do not contact because they are separated by the nasals. At the contact with the maxilla, the posterior part of the premaxilla bears a notch to accommodate the corresponding large dentary tooth; this is especially visible in right lateral view. Some pits are present in the lateral surface. Each premaxilla contains at least five teeth (although none is preserved). The preserved alveoli are as large as most of the maxillary alveoli and separated, with the third and fourth being the largest ones in SM-2023-1-16. The alveoli are circular, and the premaxillary toothrow is curved anteriorly.

Maxilla (Figs 2A, C–E, 4A–E, G, 11A–E, G, 12A, 13A–D): The two maxillae contact ventrally in an anteroposteriorly straight suture, whereas they are separated dorsally by the nasals, also in an anteroposteriorly straight suture. The triple junction between the maxilla, the premaxilla, and the nasal is situated at the level of the first maxillary alveolus. The contact with the jugal is curved

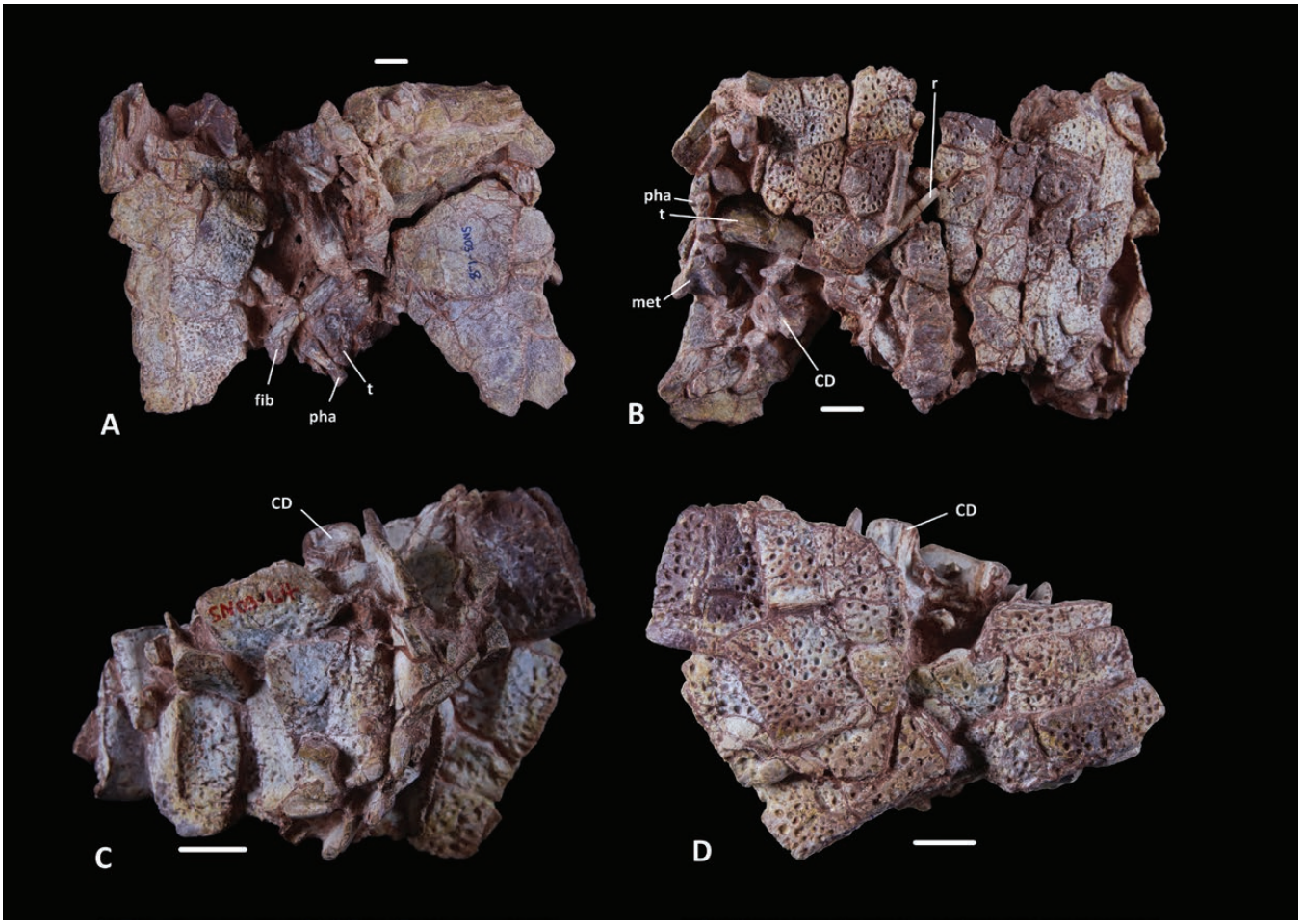

Figure 7. SM-2021-1-99 and SM-2021-1-101: caudal vertebrae and limb bones in dorsal (A, C) and ventral (B, D) views. Abbreviations: CD, cervical vertebra; fib, fibula; met, turtle metatarsal; pha, phalanx; r, rib; t, tibia. Scale bars: 1 cm.

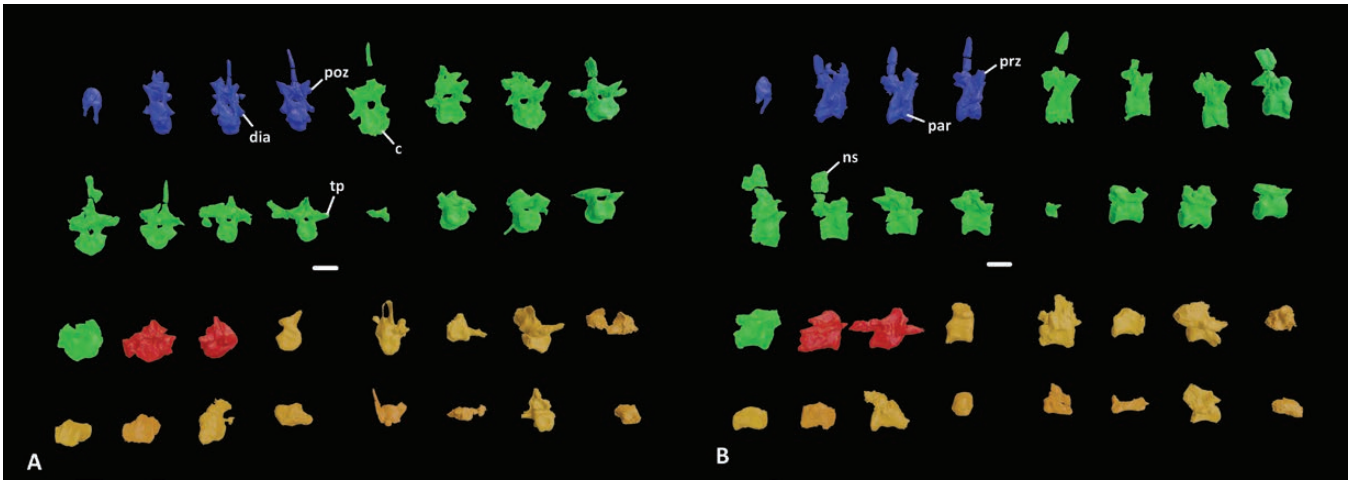

Figure 8. Three-dimensional reconstruction of *SM-2021-1-97/101* vertebrae in anterior (A) and posterior (B) views. Blue vertebrae are cervical, green are dorsal, red are sacral, and orange are caudal. Abbreviations: c, centrum; dia, diapophysis; ns, neural spine; par, parapophyis; poz, postzygapophysis; prz, prezygapophysis; tp, transverse process. Scale bars: 3 cm.

anteriorly to oblique in lateral view. Medially, there is a suture with the ectopterygoid, which is also curved anteriorly. In lateral view, a depression for the insertion of a dentary tooth can be seen at the level of the sixth–seventh maxillary alveoli, where the maxilla curves medially. Dorsally, the maxilla has two planes: one directed dorsomedially to ventrolaterally, and one oriented anteroposteriorly and flat dorsoventrally: the specimens have an altirostral skull. The contact between these two planes is directed

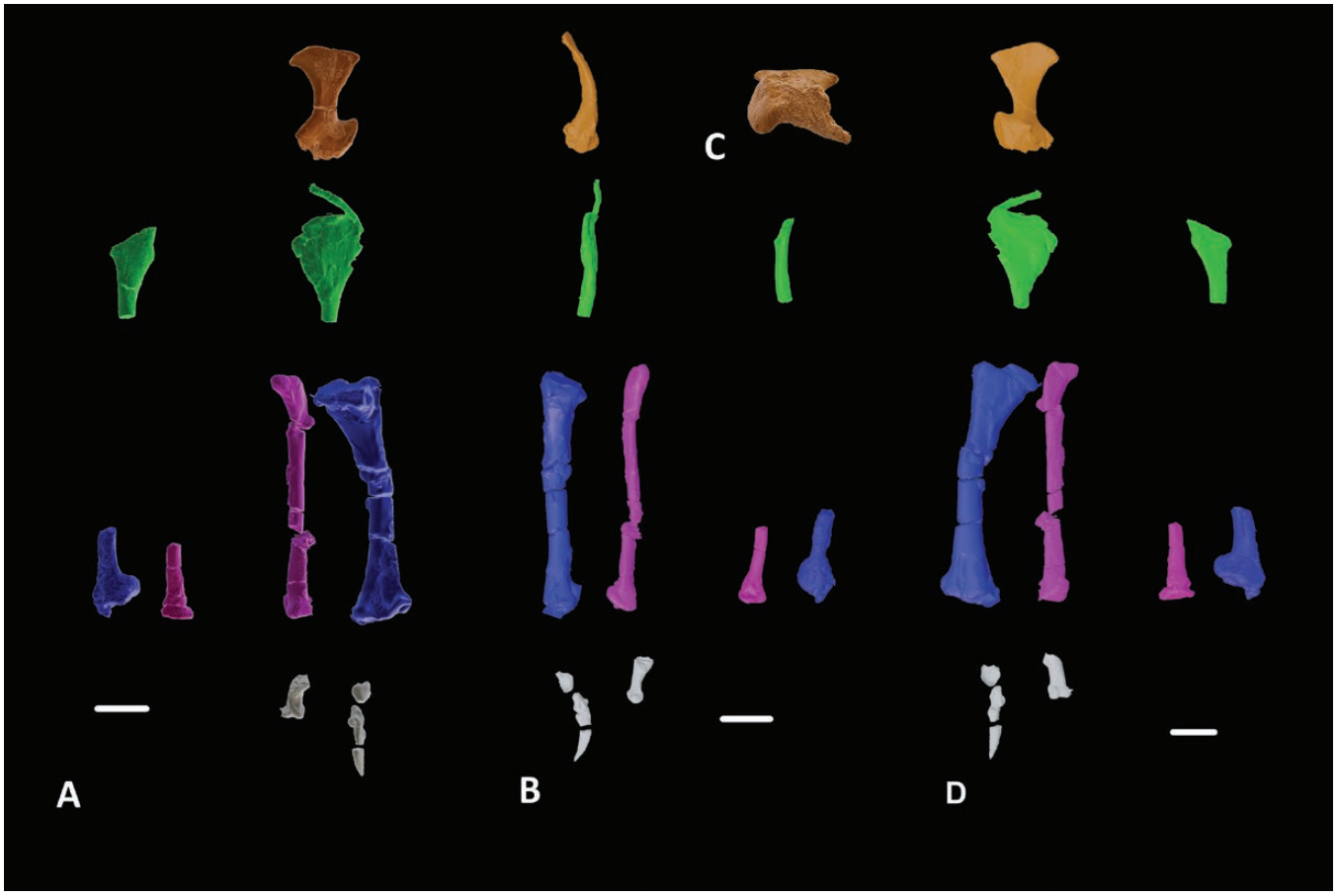

Figure 9. Three-dimensional reconstruction of *SM-2021-1-97/101* limb bones and girdles in dorsal (A), lateral (B), and ventral (D) views. C, articular surface of the coracoid. Colour key: orange, coracoid; green, pubis; purple, fibula; blue, tibia; white, digit and ungual. Scale bars: 2 cm.

posteromedially until the most developed caniniform maxillary tooth (fourth alveolus in SM-2021-1-97) or the very marked lateral bulge of the maxilla (sixth alveolus on SM-2023-1-16), then it seems to widen again laterally. The lateral margin of the maxilla forms two convex waves, with the maximum curvature at the level of the fourth and penultimate maxillary alveoli. Ventrally, the contact with the palatine is anteriorly convex, and the maxilla constitutes the anterior and anterolateral margin of the suborbital fenestra. The ventral surface is smooth. In SM-2021-1-97/99, there are at least five anterior maxillary teeth that are preserved, with the largest one being the fourth. The fifth alveolus is smaller than the third or the fourth one. All those alveoli are circular in cross-section. From the preserved parts of SM-2023-1-16, which is better preserved in this area, it can be assessed that the maxilla contains ≥10 teeth. The largest anterior alveoli, although separated, are the third and the fourth ones, but the fifth one is almost the same size as the third one. A diastema is present between alveoli five and six, probably to accommodate the enlarged dentary tooth. Then the alveoli globally decrease in size again posteriorly; they are lateromedially compressed and closely spaced. In ventral view, the alveolar rows globally diverge posterolaterally, with a concavity at the level of the fifth–sixth alveolus. The largest tooth is preserved on each side, in addition to some other fragments of other teeth. Those are caniniform teeth, with no particular carinae or ridges, and they are not compressed lateromedially.

Nasal (*Figs 2A, E, 4A, C, E, G, 11A, E, 13A, D*): The nasals are paired and elongated anteroposteriorly (no more than 1.5–2 cm). The suture with the maxilla and the premaxilla is straight anteroposteriorly. The contact between the frontal and the nasals is V-shaped, with the frontal projecting anteriorly in the nasals. The anterior end of the nasal constitutes the posterior and medial margin of the internal nares. In SM-2023-1-16, the nasals form a complete internarial bar. The posterior end of the nasals is squeezed between the contact with the frontal and the anterior projections of the prefrontals laterally in SM-2021-1-97 or the anterior projection of the lacrimal in SM-2023-1-16. The nasal does not contact the lacrimal in SM-2021-1-97, but it does in SM-2023-1-16. The bone is not visible in ventral view.

Lacrimal (*Figs 2A, C, D, 4A–E, G, 11A, D, 13A, C, D*): The lacrimal is triangular in shape, with one tip directed anteromedially. The posterior curved margin forms a part of the anterior margin of the orbit. The medial side is bordered by the prefrontal, whereas the lateral side contacts the posterior part of the maxilla. The lacrimal is shorter anteroposteriorly than the prefrontal in SM-2021-1-97, whereas it is of the same size in SM-2023-1-16. The ventral surface is too damaged to be described. In SM-2023-1-16, the lacrimal forms the dorsal border of the antorbital fenestra and connects with the maxilla and the jugal ventrally.

Jugal (*Figs 2A, C, E, F, 3A–C, G, 4, 11A, C–E, G, 13A, C, D*): The jugal is elongate and plate-like (taller than wide). Anteriorly,

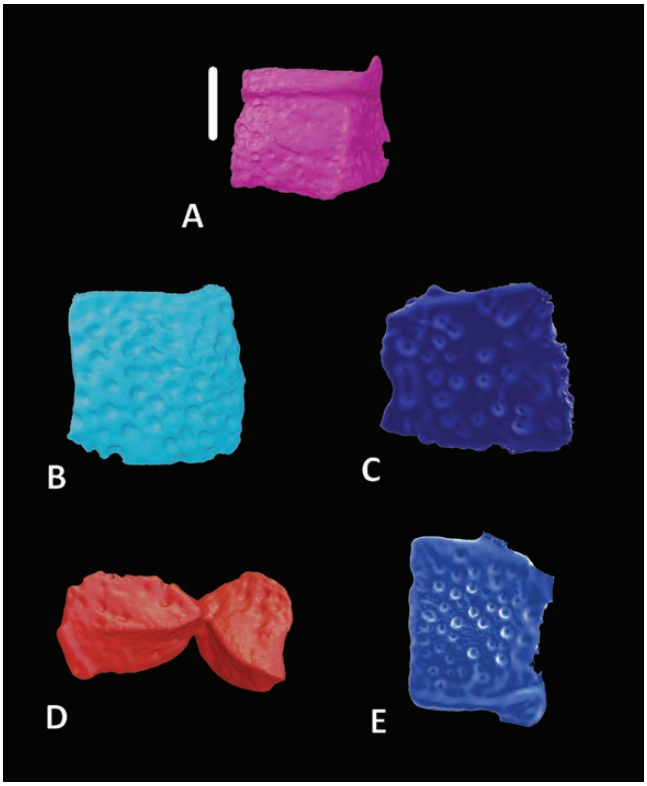

Figure 10. Three-dimensional reconstruction of *SM-2021-1-97/101* osteoderms. A, dorsal osteoderm of the cervical region. B, C, dorsal (B) and ventral (C) osteoderm of the sacral region. D. E, dorsal (D) and ventral (E) osteoderm of the caudal region. Scale bar: 2 cm.

it is directed straight anteroposteriorly, whereas posteriorly it curves mediolaterally (near the contact with the quadratojugal). The jugal sends a convex process to connect with the maxilla on the lateral side, at the same level as the lacrimal, extending to the penultimate alveolus in SM-2023-1-16. In both specimens, a crest followed by a depression can be seen, with both being directed anteroposteriorly. Posteriorly, the bone connects medially with the quadratojugal almost all the way to the posterior extremity of the skull and almost participates in the articulation with the mandible. The jugal also forms most of the lateral edge of the orbit; however, it does not form a dorsal bulge in this region. Behind the orbit, the jugal has a dorsomedially angled process, which sutures with the postorbital in an anterolaterally curved suture. The posterior margin of this contact, together with the preserved posterior part of the jugal, forms the lateral and anterolateral margins of the infratemporal fenestra. The contact with the quadratojugal is straight, and no foramina or special ornamentation can be seen in dorsal view.

Prefrontal (Figs 2A, C, D, 4A–E, G, 11A, C–E, G, 13A, C, D): The prefrontal is squeezed between the lacrimal laterally and the frontal and the nasal medially, both with straight sutures. Its anteromedialmost part connects with the posterolateralmost part of the nasal. It also connects anteriorly with the maxilla in a lateromedially straight suture. It is wider anteriorly than posteriorly in SM-2021-1-97, whereas it wider posteriorly than anteriorly in SM-2023-1-16. It makes most of the medial margin of the orbit. Ventrally, it is damaged but connects with the palatine through a transversely expanded prefrontal pillar. Those pillars meet at the midline, although this might be attributable to taphonomic deformation.

Frontal (Figs 2A, D, 4A, C–E, G, 11A, C–E, 13A, C, D, 14A, F): The frontal forms a bridge between the rostrum and the postorbital region of the skull and makes part of the posteromedial margin of both orbits. Those margins are dorsally raised. Anteriorly, it connects with the nasals in a V-shaped suture, with an anteriorly projected process of the frontal. Posteriorly, it sutures with the parietal and the postorbitals in zigzagged sutural surfaces that are straight overall. Laterally, it does not contact with the lacrimal but with the prefrontal anteromedially. It forms the anteromedial margin of the supratemporal fenestra. The dorsal surface of the frontal is slightly concave and bears a sagittal crest. It is not thick dorsoventrally. In SM-2021-1-97/99, the ventral surface bears cristae cranii frontales, which delimit the olfactory tract (Iordansky 1973; Fig. 2B).

Postorbital (Figs 2A, C, D, 4A–E, G, 11A, C–E, 12B, C, 13A, C, D, 14A, C, D, F): The postorbital forms the posterior margin of the orbit, the anterolateral margin of the supratemporal fenestra, and the anterior margin of the infratemporal fenestra. It has a T-shape, with one branch directed medially, another one posteriorly, and the final one ventrally. Medially, it contacts only the frontal. Posteriorly, the suture with the squamosal is straight (curved posteriorly in SM-2023-1-17) and is situated rather anteriorly, at the level of the middle of the supratemporal fenestra. Laterally, the postorbital sends a long projection connecting with the jugal. As a result, it forms most of the anterior margin of the infratemporal fenestra.

Parietal (Figs 2A, F, 4A, F, G, 11A, E, 13A, E, 14A, E): This single bone is part of the skull roof. It has a rectangular shape with depressed sides, like an hourglass. It is less wide mediolaterally than the posterior part of the frontal in SM-2021-1-97 but as wide as in SM-2023-1-16. Its anterior edge is smaller than its posterior one in SM-2021-1-97 and SM-2023-1-17 as well because it widens abruptly posterior to the supratemporal fenestrae, but those edges are the same size in SM-2023-1-16. Laterally, the parietal forms the medial margin of both supratemporal fenestrae, extending ventrolaterally. Those margins are elevated dorsally. The parietal also bears a sagittal crest on its posterior part, aligned with the one of the frontal. On the posteromedial corner of the supratemporal fenestra, the anterior temporal foramen (or orbitotemporal foramen; Kuzmin *et al.* 2021) can be seen on each side in SM-2023-1-16. The parietal contacts the frontal anteriorly, the supraoccipital posteriorly, and the squamosal laterally. Within the supratemporal fossa, the parietal contacts the quadrate and the laterosphenoid. In SM-2023-1-17, the suture with the squamosal is raised, making a continuous ridge with the raised medial margin of the supratemporal fenestra.

Squamosal (Figs 2A, C, D, F, 4A, C, D, G, 11A, D, F, 12B, C, 13A, D, E, 14A, C–E): The squamosal is T-shaped and forms the posterolateral corner of the skull roof. It contacts the quadrate anteriorly to the external auditory meatus and the otoccipital posteriorly in SM-2021-1-97 and SM-2023-1-16. This suture is straight anteroposteriorly. The anterior process connecting

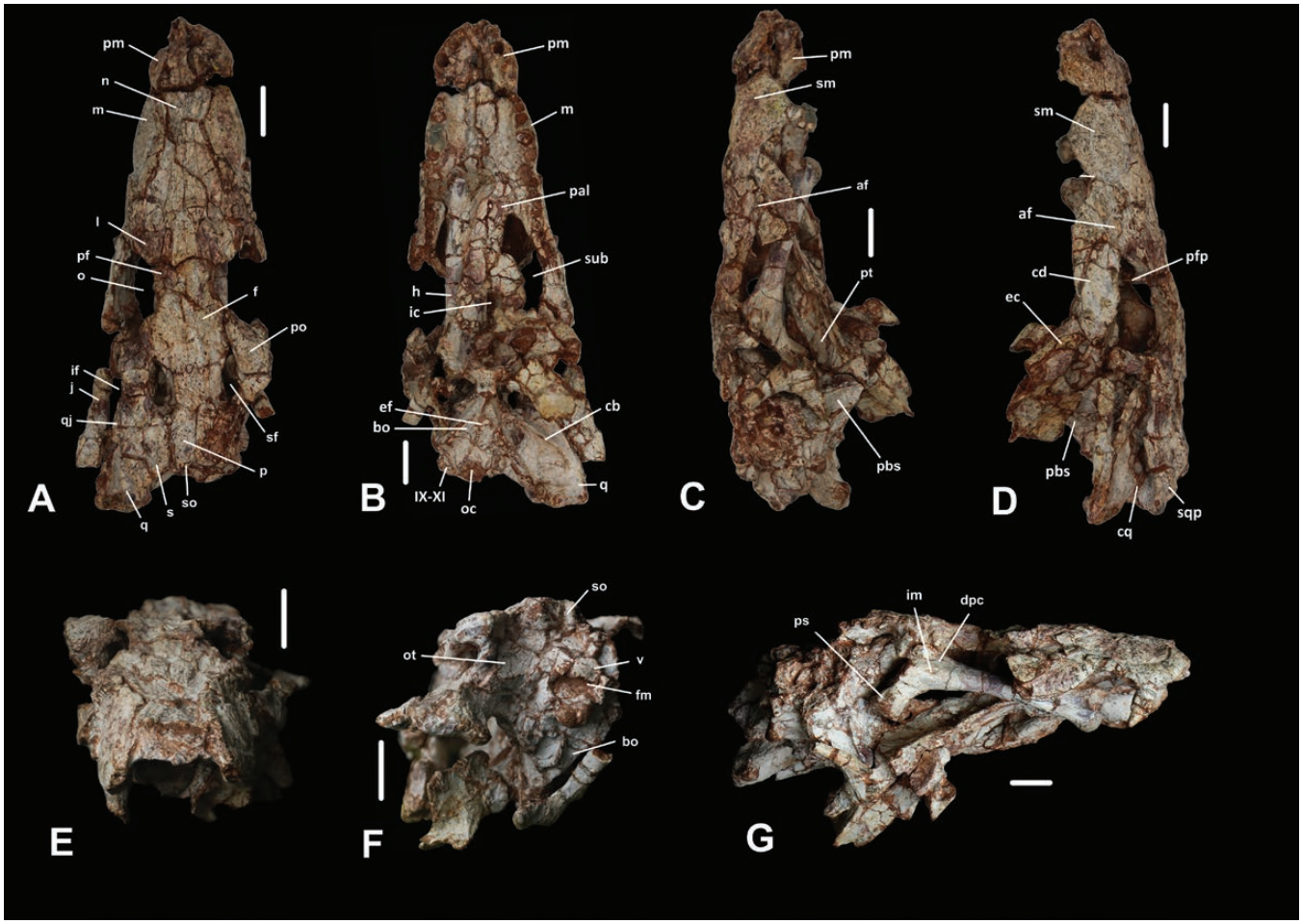

Figure 11. SM-2023-1-16 in dorsal (A), ventral (B), lateral (C, D), anterior (E), posterior (F), and ventrolateral (G) views. Abbreviations: IX–XI, foramen for cranial nerves IX–XI; af, antorbital fenestra; bo, basioccipital; cb, crest B; cd, crest/depression on the jugal; cq, cranioquadrate passage; di, depression for the insertion of a dentary tooth; dpc, deltopectoral crest; ef, eustachian foramen; f, frontal; fm, foramen magnum; h, humerus; ic, internal choana; if, infratemporal fenestra; im, insertion for the muscle teres major; j, jugal; l, lacrimal; m, maxilla; n, nasal; o, orbit; oc, occipital condyle; ot, otoccipital; p, parietal; pal, palatine; pf, prefrontal; pfp, prefrontal pillar; pm, premaxillary; po, postorbital; ps, proximal extremity; pt, pterygoid; q, quadrate; qj, quadratojugal; s, squamosal; sbf, suborbital fenestra; sf, supratemporal fenestra; sm, sulcus on the maxilla; so, supraoccipital; sqp, squamosal process; v, vertebrae remains. Scale bars: 1 cm.

with the postorbital is long and forms up to two-thirds of the posterolateral margin of the supratemporal fenestra. Posteriorly, the contact with the parietal is straight anteroposteriorly (curved laterally in SM-2023-1-17) and raised dorsally, forming a crest. In the posteriormost part, the squamosal contacts the otoccipital ventrally; it forms the dorsolateral part of the skull. Posterolaterally, the squamosal forms an elongated process that is directed posterolaterally and in the same plane as the one of the cranial table in SM-2021-1-97 or ventrally in SM-2023-1-16, but this is probably a taphonomic artefact. The squamosal has a longitudinal groove for the muscles of the external ear flap located dorsally to the external auditory meatus in lateral view.

Quadratojugal (Figs 2A, C, D, 4A, C–E, G, 11A, 12B, C, 13A, D): This bone extends posteriorly from the dorsomedial corner of the infratemporal fenestra. The posterior part is thin and squeezed between the quadrate medially and the jugal laterally. It extends all the way to the posterolateralmost part of the skull and participates in the articulation with the mandible. The suture with the jugal is straight in SM-2023-1-16 and curved medially in SM-2021-1-97, whereas the suture with the quadrate is curved laterally. The bone is smooth dorsally, thin, and plate-like, and of the same width all the way; it is also higher mediodorsally than lateroventrally.

Quadrate (Figs 2A–D, F, G, 3G, 4, 11A, D, F, 12B, C, 13, 14B): The quadrate has a complex shape. Anteriorly, it does not reach the infratemporal fenestra, but it reaches the ventral margin of the supratemporal fenestra and contacts the parietal. Dorsally, it contacts the squamosal anteriorly to the external auditory meatus in SM-2021-1-97/99 and in SM-2023-1-16. The suture with the quadratojugal is straight anteromedially to posterolaterally in SM-2021-1-97/99, whereas it is curved laterally in SM-2023-1-16. The quadrate should contact the pterygoid ventrally, but the area is too damaged on all specimens to describe. Posteriorly, the contact with the otoccipital is straight, situated posteriorly to the external auditory meatus, and posteroventrally the quadrate is also connected to the basioccipital in SM-2021-1-97/99 (although this is probably a taphonomic artefact) but not in SM-2023-1-16. The subtympanic foramen, the oval opening

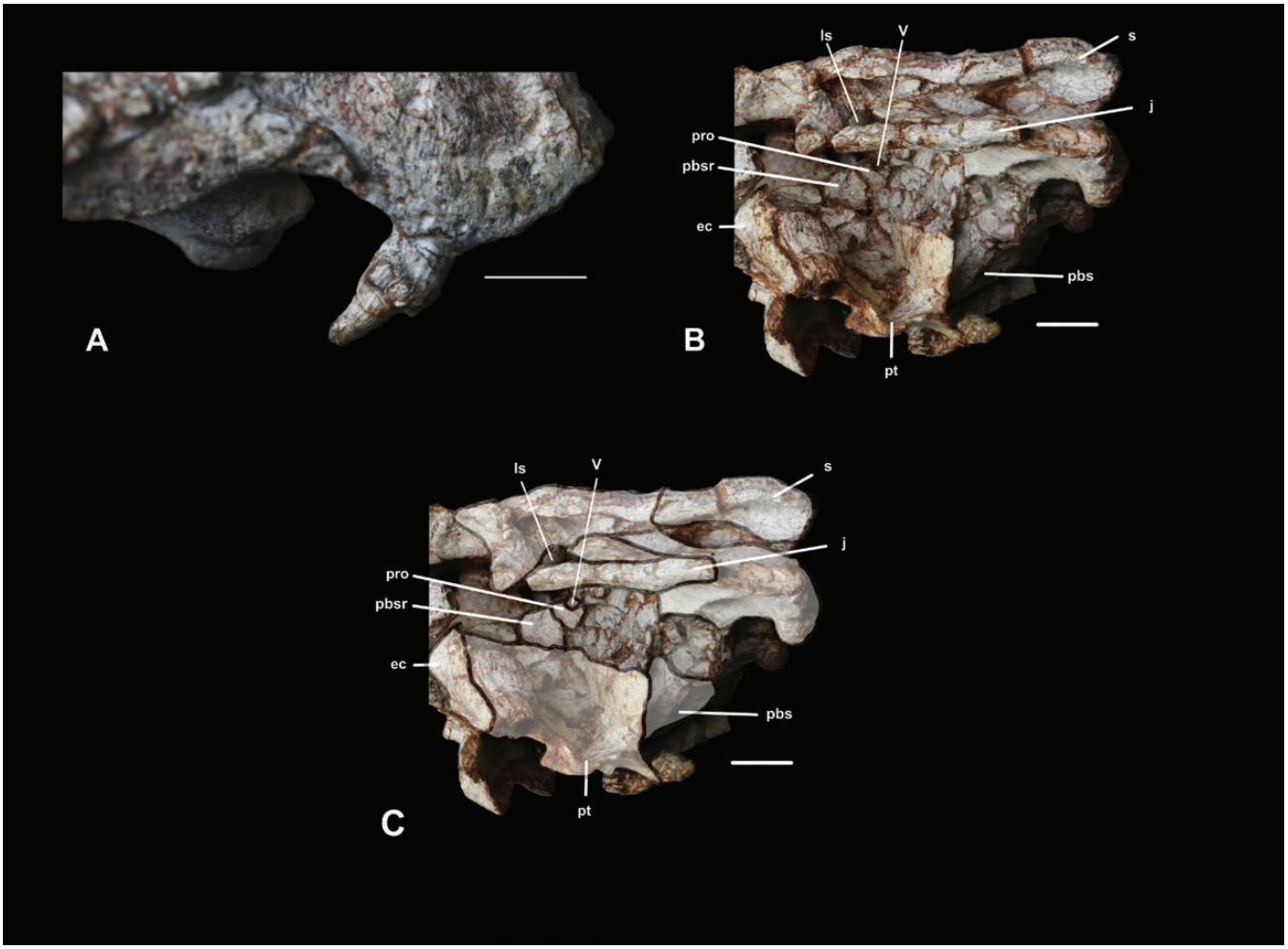

Figure 12. Details of SM-2023-1-16: tooth (A), braincase region (B), and outlines of the bones in the braincase region (C). Abbreviations: V, foramen for cranial nerve V; ec, ectopterygoid; j, jugal; ls, laterosphenoid; pbs, parabasisphenoid; pbsr, basisphenoid rostrum; pro, prootic; pt, pterygoid; s, squamosal. Scale bars: 1 cm.

leading into the cavity within the quadrate, can be observed at the anteromedial margin of the quadrate on SM-2021-1-97/99. The foramen aërum can be seen on the left quadrate of SM-2021-1-97/99; it is located laterodorsally to the medial condyle. Crest B (Iordansky 1973) is extremely developed ventrally, extending closely to the quadrate–quadratojugal suture posteriorly and curving anteromedially to medially. Posteriorly, the quadrate articulates with the mandible. Its surface is divided into two hemicondyles laterally and medially, equal in size. The quadrate is bordered almost all the way by the squamosal and the otoccipital on the medial side and by the quadratojugal on the lateral side. Medially, it sutures with the pterygoid and probably the other bones of the braincase, but the area is too damaged in all specimens to be described. This bone is 1–1.5 cm tall in cross-section and curved dorsally.

Supraoccipital (Figs 2A, F, 4A, F, 11A, F, 13A, E, 14E): This bone is triangular in shape in posterior view. It is exposed in dorsal view. Laterally, it connects with the otoccipital. It also does not participate in the formation of the foramen magnum in SM-2021-1-97. It is more difficult to assess in SM-2023-1-16 and SM-2023-1-17 because those areas are covered by other fragments.

Otoccipital (Figs 2F, 4A, C, D, F, G, 11F, 13E, 14E): This bone connects laterally with the quadrate, medially with the supraoccipital, and dorsally with the squamosal in a straight to curved contact. In posterior view, it extends laterally to the lateral edge of the skull (not in SM-2023-1-17). On SM-2021-1-97 there are three foramina: the lateralmost one is for the internal carotid artery, and the two others are the two exits for cranial nerves XII. On SM-2023-1-16, a foramen can be seen dorsolaterally from the occipital condyle; it is the foramen for the cranial nerves IX–XI. The otoccipital also connects with the basioccipital ventrally. The whole bone is plate-like and gradually protrudes caudally with an angle of ~30° to the vertical axis, showing a small ridge directed mediolaterally.

Basioccipital (Figs 2B, D, F, G, 4A, B, F, 11B, F, 13B, E): The basioccipital sutures laterally with the otoccipital (in posterior view), the quadrate (in lateral view), and maybe the pterygoid posteroventrally (in SM-2021-1-97/99). In this specimen, the separation between the parabasisphenoid and the basioccipital was very difficult to assess; therefore, it might also be that the basioccipital is separated from the pterygoid by the parabasisphenoid. It bears a median crest and two

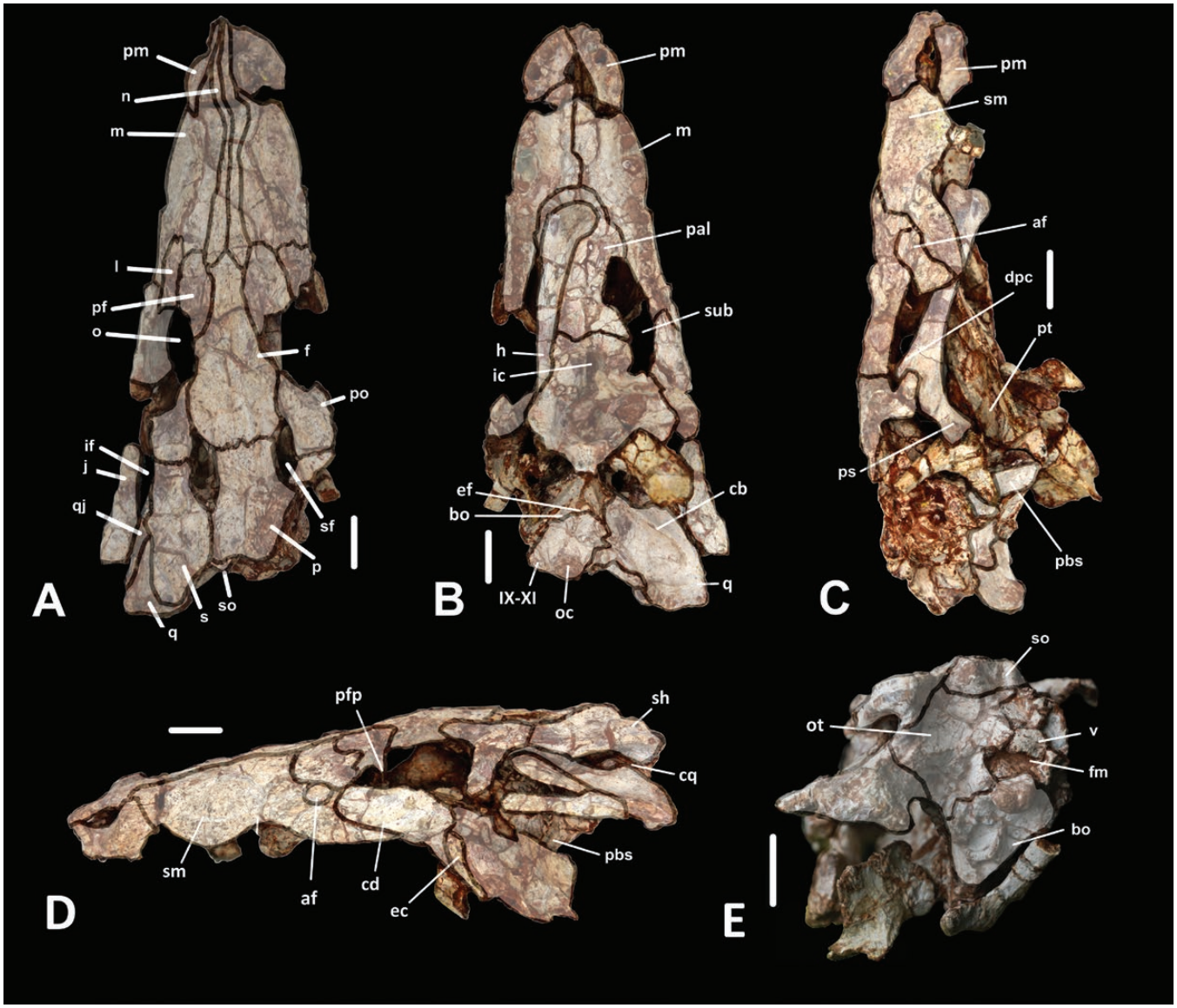

Figure 13. Outlines of the bones of SM-2023-1-16 in dorsal (A), ventral (B), lateral (C, D), and posterior (E) views. Abbreviations: IX–XI, foramen for cranial nerve IX–XI; af, antorbital fenestra; bo, basioccipital; cb, crest B; cd, crest/depression on the jugal; cq, cranioquadrate passage; dpc, deltopectoral crest; f, frontal; fm, foramen magnum; h, humerus; ic, internal choanae; if, infratemporal fenestra; j, jugal; l, lacrimal; m, maxilla; n, nasal; o, orbit; oc, occipital condyle; ot, otoccipital; p, parietal; pal, palatine; pbs, parabasisphenoid; pf, prefrontal; pfp, prefrontal pillar; pm, premaxillary; po, postorbital; ps, proximal surface; pt, pterygoid; q, quadrate; qj, quadratojugal; s, squamosal; sf, supratemporal fenestra; sh, squamosal 'horn'; sm, maxillary sulcus; so, supraoccipital; sub, suborbital fenestra; v, vertebrae remains. Scale bars: 1 cm.

lateral tuberosities, and the median pharyngeal foramen is clearly visible ventrally to the central crest. The basioccipital is only preserved posteriorly; it has a plate-like shape directed anterolaterally to posteromedially. The occipital condyle is directed posteroventrally.

Palatine (Figs 2B, G, 3D, E, 4B, G, 11B, 13B): The palatine connects with the maxilla in an anteriorly convex suture in SM-2021-1-97/99 and SM-2023-1-16. The posterior region is heavily damaged and remodelled, but it does not include the choana in SM-2021-1-97/99 (Fig. 3G). However, this could be the case in SM-2023-1-16, where the palatine would form its anterior margin, but because of the poor state of preservation it is difficult to assess. The suture with the pterygoid is also anteroposteriorly straight immediately anterior to the internal choana. The paired palatines are flat when they meet at the midline. In ventral view, the lateral margins of the palatines are parallel and straight in SM-2021-1-97/99. This is not the case in SM-2023-1-16, but might more probably be attributable to a deformation induced by the humerus. The ventral surface is smooth and raised dorsally in SM-2023-1-16. The vomer cannot be seen.

Pterygoid (Figs 2B, D, F, G, 3C–F, 4B–D, F, G, 11C, 12B, C, 13B, C): The pterygoid is sutured to the palatine anteriorly, the ectopterygoid laterally, and the basioccipital posteriorly. Each pterygoid makes a straight connection with the corresponding

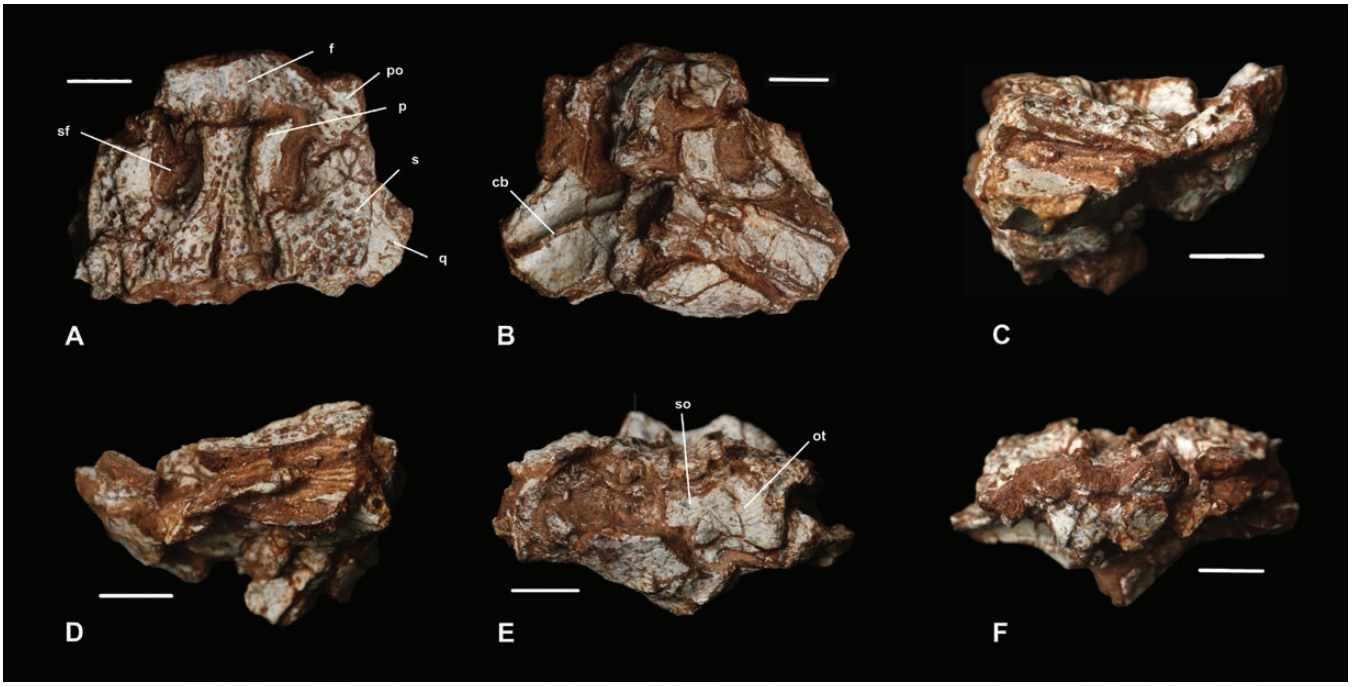

Figure 14. SM-2023-1-17 in dorsal (A), ventral (B), lateral (C, D), posterior (E), and anterior (F) views. Abbreviations: cb, crest B; f, frontal; ot, otoccipital; p, parietal; po, postorbital; q, quadrate; s, squamosal; sf, supratemporal fenestra; so, supraoccipital. Scale bars: 1 cm.

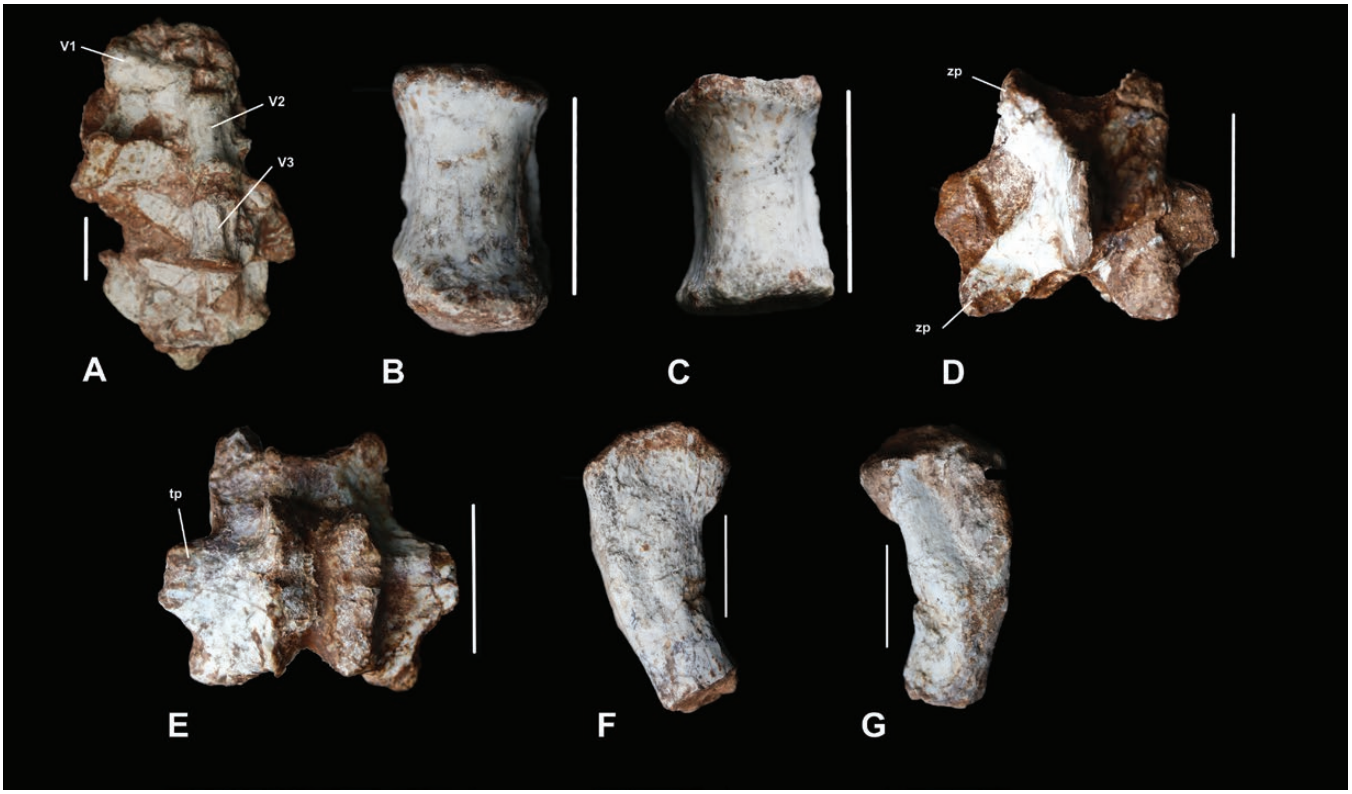

Figure 15. Different postcranial parts (SM-2023-1-17): three linked vertebral centra (A), two vertebral centra (B, C), upper part of a vertebra in dorsal (D) and ventral (E) views, and proximal part of limb bone in anterior (F) and posterior (G) views. Abbreviations: tp, tranverse process; V1, vertebra 1; V2, vertebra 2; V3, vertebra 3; zp, zygapophysis. Scale bars: 1 cm.

ectopterygoid and tends to be more curved ventrally at that point. The internal choana is ovoid, bordered by prominent anterior margins in ventral view, and has no midline process. It is totally enclosed by the pterygoids in SM-2021-1-97/99 (its status is unknown in SM-2023-1-16) and is anterior to the posterior margin of the suborbital fenestra. Anteriorly, a median

process of the pterygoid extends to contact the palatine and forms the ventral edge of the interorbital septum. The pterygoid is smooth on all surfaces except on the lateralmost sides.

Ectopterygoid (Figs 2B, D, 3C, D–F, 4B, C, F, G, 11D, 12B, C, 13B, D): This bone contacts the jugal and the maxilla laterally and the pterygoid medially (forming the pterygoid flange). The triple junction between the maxilla, the jugal, and the ectopterygoid is situated at the middle of the anterior process of the ectopterygoid in SM-2021-1-97/99. The ectopterygoid could constitute the posterolateral margin of the suborbital fenestra, but it cannot be assessed with certainty owing to the poor preservation of this area in this specimen. However, it does not ascend on the medial margin of the postorbital bar. In SM-2023-1-16, the ectopterygoid forms the posterolateral margin of the suborbital fenestra, and its anterior process contacts the posteriormost maxillary alveolus. This bone is curved ventrally and laterally. In both specimens, the ectopterygoid extends up to the preserved posteriormost part of the pterygoid wing.

Laterosphenoid (Fig. 12B, C): The dorsoposterior ridge of the laterosphenoid connects with the parietal. The ventralmost part of the bone contacts the quadrate, forming the foramen for cranial nerve V.

Parabasisphenoid (Figs 11C, D, 12B, C, 13C, D): The parabasisphenoid is complex. Anteriorly, the parabasisphenoid rostrum is short and not dorsoventrally elevated. It does not contact the laterosphenoid; however, it does contact the prootic and the pterygoid. Posteriorly, it has a plate-like shape directed anterolaterally to posteromedially. It contacts the pterygoid ventrally, the quadrate dorsally, and the basioccipital posteriorly, encircling the pharyngeal foramen. This part also bears a crest directed anteroventrally to posterodorsally.

Prootic (Fig. 12B, C): This small bone sutures with the laterosphenoid posteriorly on the posterior margin of the foramen and the parabasisphenoid rostrum anteriorly.

Mandible (Figs 2B, G, 3, 4)

There is no external mandibular fenestra. Both coronoids are missing. Overall, the mandible is ornamented with circular to ovoid pits and grooves.

Dentary (Figs 2B–E, G, 3B, C, 4B–G): This bone is the only tooth-bearing element of the mandible, with ≥13 alveoli. The two rami separate at the level of the fifth dentary tooth and are firmly sutured anteriorly. The symphyseal region remains wide anteriorly and is U-shaped at its anteriormost point. In medial view, the dentary is thin dorsoventrally and forms an acute angle anteriorly. Ventrally and dorsally, the medial suture with the splenial is oblique, directed posterolaterally to anteromedially. The dentary remains uniform in width up to the point of divergence, where it begins to taper off. Posteriorly, the dentary connects dorsally with the surangular, from the end of the toothrow, and ventrally with the angular at its posteriormost part. The ventral surface is smooth, and anteriorly it is curved dorsally. The lateral side shows no groove ventral to the tooth row. In lateral view, the dorsal margin is sinusoidal, marked by two sets of waves that culminate at the level of the 3rd/4th and 11th/12fth dentary alveoli. There is also a medial depression to accommodate the largest caniniform maxillary tooth at the level of the 9th dentary alveolus, especially visible on the left side. In terms of size, alveoli 4–10 and 13 are relatively small, whereas the 3rd one is the largest, and the 11th and 12th are also large. Alveoli 4–7 and 8–10 are closely spaced, whereas there is a larger space between alveoli 7 and 8. The ventral margin of the dentary is straight anteroposteriorly.

Splenial (Figs 2B, G, 3C, 4): The splenial is most exposed medially; it forms a vertical plate that sutures with the dentary and with the other splenial at the midline anteriorly. It reaches up to the fifth dentary tooth and is not exposed ventrally. Posteriorly, it becomes thin and plate-like along the medial surface of the dentary (even becoming the medial wall for the last posterior dentary alveoli, from the 11th one) until it disappears posteriorly without meeting the angular or the surangular. In posterior view, the circular foramen intermandibularis oralis is present at the point where the two splenials diverge (not on the medial sides) and is small. The mandibular symphysis completely involves the first eight alveoli. The dorsal exposure of the splenial is strictly triangular in shape and makes up more than one-third of the mandibular symphysis. The dorsal surface bears rugosities, whereas the medial surface is smooth and flat.

Angular (Figs 2B, D, F, G, 3A, B, H, 4B–D, 4F, G): The angular is the most ventral mandibular element (approximately half of the total length of the mandible). In lateral view, it is elongated, and posteriorly it is curved dorsally. Medially, the angular sutures with the dentary, the surangular, and the articular to form a huge medial depression (adductor chamber; Iordansky 1973). Dorsally, it sutures with the dentary anteriorly and the surangular posteriorly, finishing as a sharp process lateral to the retroarticular process and curving inwards and upwards. Only the lateral surface is ornamented; the others are smooth. The area of insertion of the muscle pterygoideus is not very developed and is visible only in the posteroventral margin of the angular.

Surangular (Figs 2C, F, 3A–C, G, H, 4): This bone is robust and elongated. Anteriorly, its dorsal process might extend between the dentary and the splenial, but the preserved parts of the specimen show only a contact between the surangular and the dentary anteriorly. Posteriorly, it tends to curve dorsally and sutures with the angular for the rest of its length and medially with the articular. It also becomes more plate-like. This suture is linear anteriorly, and posteriorly it curves dorsally. The bone also curves medially and forms the lateral margin of the articular fossa. Laterally to this, there is a short ridge oriented anteroposteriorly, forming a depression. The dorsal surface is convex, not ornamented, and flattens before the glenoid surface. On the lateral surface, there is a ridge directed posterodorsally to anteroventrally.

Articular (Figs 2A, B, D, F, G, 3G, H, 4A, B, D–F): The articular is the most posterior element of the mandible. It has two dorsal surfaces separated by a ridge oriented lateromedially. The anterior surface articulates with the quadrate; the ridge helping to

stabilize this articulation as its posterior wall is tall and dorsally edged. The articular fossa is divided into a lateral and a medial portion of equal size by a small ridge oriented anteroposteriorly. The posterior surface (retroarticular process) is concave overall and paddle shaped. It seems to taper posteriorly, but the most posterior part is broken on each side. Ventromedially, the articular forms the posteromedial wall of the adductor chamber. It sutures with the surangular at its lateral margin and with the angular at its ventral margin.

Dentition (Figs 2C–E, H, I, 4C–E, G, 12A): A large maxillary caniniform tooth is preserved on each side of the skull. It is conical and slightly curved lingually. The base of the tooth crown is ovoid in cross-section, and the apex is pointed. There are no carinae or crenulations visible in SM-2021-1-97/99, whereas there are carinae but with no crenulations in SM-2023-1-16. The enamel, although damaged, shows thin and basoapically directed striations. This morphotype corresponds to the 'pseudocaniniform' morphotype described previously (Schwarz and Salisbury 2005, Lauprasert *et al.* 2011, Tennant *et al.* 2016). The upper dentition also preserves a smaller tooth, on the left side immediately anterior to the big caniniform tooth. On the mandible, a lot more teeth are present, throughout the tooth row, and they belong to both the 'pseudocaniniform' and the 'lanceolate-shaped' morphotypes (Schwarz and Salisbury 2005, Lauprasert *et al.* 2011, Tennant *et al.* 2016). The anterior teeth are strongly procumbent, and the third one is well developed, as are the 11th and 12th. The third and fourth dentary alveoli are confluent.

Axial skeleton (Figs 5–8, 10, 15A–E)

Most crocodylians possess eight cervical vertebrae, 16 dorsals (lumbar included), two sacrals, and 30–40 caudals (Mook 1921, Gomes de Souza 2018). Furthermore, the cervical and the first three dorsal vertebrae exhibit a similar morphology, whereby the parapophysis and the diapophysis are separated. Then, from the fourth dorsal vertebra, the parapophysis and the diapophysis are fused, forming the transverse processes connecting with the ribs (Gomes de Souza 2018). In *SM-2021-1-97/101*, there are ≥32 vertebrae. Given that the area of transition between the cervicals and the anterior dorsals (SM-2021-1-98; Fig. 5) and between the posterior dorsals and the sacrals (SM-2021-1-100; Fig. 6) are preserved, we can establish the following: *SM-2021-1-97/101* preserves 4 cervicals (5th–8th), 12 dorsals (1st–8th in the anterior part and 13th–16th in the posterior part), 2 sacrals ,and 14 caudals (only the 1st can be numbered). The proatlas/atlas and axis are missing. All the preserved vertebrae seem to be amphicoelous. All processes are described based on the nomenclature of Gomes de Souza (2018).

Cervicals (Figs 5A–C, E, 8): The neural arches and spines are tall, narrow, and pointed dorsally. The diapophyseal processes are longer than the parapophyseal processes. The zygapophyses are large in comparison to the centra, with the prezygapophyses being larger than the postzygapophyses. These structures become horizontal posteriorly. All the centra are amphicoelous, and the lateral sides of the centra (between the diapophyseal and parapophyseal processes) are notably depressed. The last cervical vertebra has a tall neural spine (more than two times the height of the centrum). The hypapophyses are broken, but their areas of insertion on the centrum are still visible on all centra. The diapophyseal processes gradually increase in size posteriorly, and they also migrate from the lateral side of the centrum to the lateral side of the neural arch. The parapophyseal processes do not seem to increase in size, but they also migrate dorsally, going from the lateroventral margin to the lateral side of the centrum posteriorly.

Dorsals (Figs 5B–D, 6B, C, 8): The neural spines are anteroposteriorly longer than those of the cervicals. The first dorsal vertebra has the tallest neural spine (more than two times the height of the centrum). The diapophyseal and parapophyseal processes are too damaged to be described. On the centrum of the first dorsal vertebra, the proximal part of the hypapophysis is preserved; it is half the size of the centrum. The ventral hypapophyses are either absent or too damaged to be seen from the second or third centra. The articular facets of the pre- and postzygapophyses are more horizontally oriented.

Sacrals (Figs 6, 8): There are two sacral vertebrae of the same size. The base of their neural spine is long anteroposteriorly for both. On the second vertebra, the transverse processes and their articular surfaces are more developed, probably because they are less damaged than on the second one. The costal caudalis is directed ventrally on the first sacral. The contact between the two centra is flat. The anterior articular surface of the first sacral and the posterior articular surface of the second sacral are both concave.

Caudals (Figs 6, 7B–D, 8): The first caudal vertebra is large, and its articular surfaces are concave to flat. The other ones are damaged. The second has a neural spine that is preserved; it is high dorsoventrally and long anteroposteriorly. Some of them have two horizontal ridges on the centrum, perhaps for the insertion of the chevron. A chevron is preserved; it is triangular in shape and open in the middle.

Ribs (Figs 5A, 7B): Some ribs are preserved, but it is difficult to identify to which vertebra they were attached. When those structures are preserved, the tuberculum is less developed than the capitulum. The ribs are slightly curved and are rod-like.

Pectoral girdle (Fig. 9)

Coracoid (Fig. 9): The left coracoid is preserved. This bone is convex overall. The shaft is triangular, and both ends of the bone are extended. The coracoid foramen is visible in the most proximal part. The articular surface with the scapula is flat, and the ventral part of the glenoid fossa is saddle shaped and directed posteriorly. The distal end is more developed anteriorly than posteriorly.

Pelvic girdle (Figs 6B, C, 9A, B, D)

Pubis (Figs 6B, C, 9A, B, D): The two bones are flat. The most proximal part articulating with the rest of the pelvic girdle is missing in both. Overall, it has a round shape, with a convex and narrow dorsal margin.

Forelimb (Figs 11B, C, G, 13B, C)

Humerus (Figs 11B, C, G, 13B, C): The humerus is squeezed between the anterior margin of the suborbital fenestra and the right side of the parabasisphenoid rostrum. Its deltopectoral crest is slender and placed anteroproximally. On the proximomedial side, there is a ridge that connects the deltopectoral crest and the triangular-shaped head of the humerus. The humerus is straight and not very curved or twisted. The head of the humerus is very well developed and unusual among crocodyliforms, extending posterolaterally. The articular surface is flat and decreases anteromedially to articulate with the glenoid fossa. There is also a lateral projection where the humeral head reaches the shaft. The area of insertion for the muscle teres major is visible on the posterior side. Distally, on the bicondylar articulation with the zeugopod, the medial condyle for the ulna is larger than the lateral condyle for the radius.

Hindlimb (Figs 7A, B, 9A, BD)

Tibia (Figs 7A, B, 9A, B, D): The shaft of the left tibia, although deformed taphonomically, appears to be straight anteroposteriorly and curved laterally. However, both ends of the bone are on the same plane lateromedially. The proximal articulation surface is flat, with a posterior concavity. The distal articulation surface is ovoid.

Tibia (Fig 9A, B, D): The fibula is straight and very slender. The proximal end is compressed mediolaterally. The distal articular surface comprises two articular surfaces that are flat to convex: one is posteromedial and would have articulated with the calcaneum, and the other one is distal and would have articulated with the astragalus.

Digits (Fig 9A, B, D): The preserved metatarsal is concave ventrally. The distal end is separated into two condyles, with a depression on each side laterally and medially to the hemicondyles. The preserved ungual is curved ventrally and pike shaped.

Osteoderms (Figs 5–7, 10)

The dermal armour consists of a dorsal shield composed of at least three rows of mediolaterally expanded osteoderms and a ventral shield composed of rectangular-shaped osteoderms sutured to each other. Paravertebral and accessory osteoderms could not be distinguished because of preservation issues and unknown position on the body. Given that an uneven number of osteoderm rows is not known in crocodylomorphs (Salisbury and Frey 2001, Puértolas-Pascual and Mateus 2020), *Varanosuchus* either had at least four rows of paravertebral osteoderms or at least two rows of paravertebral osteoderms and two rows of accessory osteoderms. Some osteoderms bear a longitudinal keel that does not extend on the whole surface, but it is difficult to situate them on the body. Appendicular osteoderms could not be determined with certainty.

Dorsal shield (Figs 5, 6A, B, 7A, C, 10A, B, D): The osteoderms are more expanded mediolaterally anteriorly than posteriorly, but their anteroposterior size remains the same. All osteoderms are flat or slightly arched dorsally and ornamented with circular pits, as is seen on the cranial table and the posterolateral side of the mandible. There are some spine- or peg-like processes for articulation with the more anteriorly situated osteoderm that are preserved (Fig. 10A). The articulation system is as follows: the anterior osteoderm overlaps the posterior osteoderm, and the left osteoderm tends to overlap the right one. The margins are straight.

Ventral shield (Figs 5, 6C, 7B, D, 10C, E): The ventral shield is more damaged; however, it consists of square osteoderms. There are at least two rows of osteoderms. The ornamentation is the same as the dorsal shield; it consists of flat circular pits. The ventral shield is missing in the sacral region.

Phylogenetic analyses

The analysis generated 43 most parsimonious trees and a consensus tree with a length of 1509 steps (Supporting Information, Supplementary Material S6; consistency index = 0.26, retention index = 0.58). Although the support values are low (Supporting Information, Supplementary Material S6), the main groups inside Neosuchia are retrieved and supported by numerous synapomorphies. Those results are also retrieved using the heuristic search procedure, with the same topology (1509 steps, consistency index = 0.26, retention index = 0.58), hinting at the relative robustness of our analysis.

Based on ACCTRAN optimization, we retrieve Atoposauridae *sensu* Schwarz *et al.* (2017) as a monophyletic group (including *Varanosuchus sakonnakhonensis*; Fig. 16, node 4) based on the following combination of characters: a broad oreinostral skull (character 3); little participation of the premaxilla in the internarial bar (character 4); the quadrate, squamosal, and otoccipital do not meet to enclose the cranioquadrate passage (character 49); the antorbital fenestra is much smaller than the orbit (character 67); one wave of enlarged maxillary teeth (character 79); dorsal osteoderms with a well-developed process located anterolaterally in dorsal parasagittal osteoderms (character 96); two parallel rows of dorsal osteoderms (character 97); a symmetrically developed lateral compression on the maxillary teeth (character 140); and a lacrimal that tapers ventroposteriorly and does not contact or only slightly contacts the jugal (character 229).

Furthermore, Paralligatoridae *sensu* Rummy *et al.* (2022) forms a monophyletic group (Fig. 16, node 5) defined by the following synapomorphies: no vascular opening on the dorsal surface of the postorbital bar (character 27); the medial quadrate condyle expands ventrally, being separated from the lateral condyle by a deep intercondylar groove (character 170); a sharp ridge along the lateral surface of the angular (character 219); the ulna has a wide and rounded olecranon process (character 260); and a foramen located the palatal premaxilla–maxilla suture near the alveolar border (character 320).

Eusuchians (including *Bernissartia*, Atoposauridae, Paralligatoridae, Hylaeochampsidae, and Crocodylia; Fig. 16, node 3) are also retrieved as a monophyletic group, with the following synapomorphies: the choanal groove is undivided (character 69); the cervical vertebrae are procoelous (character 92); the dorsal osteoderms have a discrete convexity on the anterior margin (character 96); there are more than two rows of dorsal primary osteoderms (character 97); and the supraoccipital is exposed in the skull roof (character 171).

Finally, the two specimens from Phu Sung are retrieved as a monophyletic group (Fig. 16, node 8), with the following synapomorphies: the dorsal part of the postorbital has an anterolaterally facing edge (character 29); the quadrate has no fenestrae (character 45); two waves of enlarged maxillary teeth (festooned; character 79); a quadratojugal with no ornamentation (character 145); the outer surface of the squamosal laterodorsally oriented is reduced and sculpted (character 168); and there is a depression on the posterolateral surface of the maxilla (character 207).

DISCUSSION

Comparisons with other close crocodylomorphs from Thailand

Cretaceous crocodylomorphs reported from Thailand are restricted for now to certain neosuchians (Buffetaut and Ingavat 1980, 1983, 1984, Lauprasert *et al.* 2007, 2009, 2011, Martin *et al.* 2014a). SM-2023-1-16 and SM2021-1 are clearly not longirostrine, hence they do not belong to *Chalawan thailandicus* Martin *et al.*, 2014a or the poorly known eusuchian from Ban Saphan Hin (Kubo *et al.* 2018). *Siamosuchus phuphokensis* Lauprasert *et al.*, 2007 and *Khoratosuchus jintasakuli* Lauprasert *et al.*, 2009 do not have an altirostral snout, meaning that at least the two most complete specimens cannot be attributed to either of these taxa. Furthermore, *Khoratosuchus* is also diagnosed by internal choanae that are also formed by the palatines, which is not the case in *SM-2021-1-97/101*. However, Lauprasert *et al.* (2011) described an atoposaurid, *Theriosuchus grandinaris* Lauprasert *et al.*, 2011 from Phu Phok (Sao Khua Formation), which possesses an altirostral snout. This taxon is diagnosed by the following unique combination of characters: nasal bone gradually wider posteriorly; weak notch at the suture between the premaxilla and the maxilla; combination of pseudocaniniform, lanceolate-shaped, and labiolingually compressed with crenulated carinae teeth; mandibular symphysis not extending beyond the seventh dentary tooth; and a slender prefrontal tapering anteriorly. SM-2023-1-16 has a prefrontal rounded anteriorly, and the only tooth preserved is a pseudocaniniform one. SM2021-1 has a nasal bone that is straight posteriorly and lanceolate-shaped and pseudocaniniform teeth that do not seem to have carinae or denticles. The prefrontal is not really tapered anteriorly but more rounded. *SM-2021-1-97/101* and SM-2023-1-16 also have a depression on the posterolateral surface of the maxilla, whereas *Theriosuchus grandinaris* does not. Furthermore, *SM-2021-1-97/101* has a compressed and vertical dentary but with a flat surface exposed dorsolaterally, whereas it is not compressed and convex in *Theriosuchus grandinaris*, and the anterior dentary alveoli are strongly procumbent in *SM-2021-1-97/101*, whereas they are not in *Theriosuchus grandinaris*. As a result, the specimens described here can be distinguished from other similar crocodylomorphs known in the Mesozoic.

The status of '*Goniopholis*' *phuwiangensis* Buffetaut & Ingavat, 1983

'*Goniopholis*' *phuwiangensis* Buffetaut & Ingavat, 1983 consists of an incomplete dentary (Fig. 17) and is considered by some

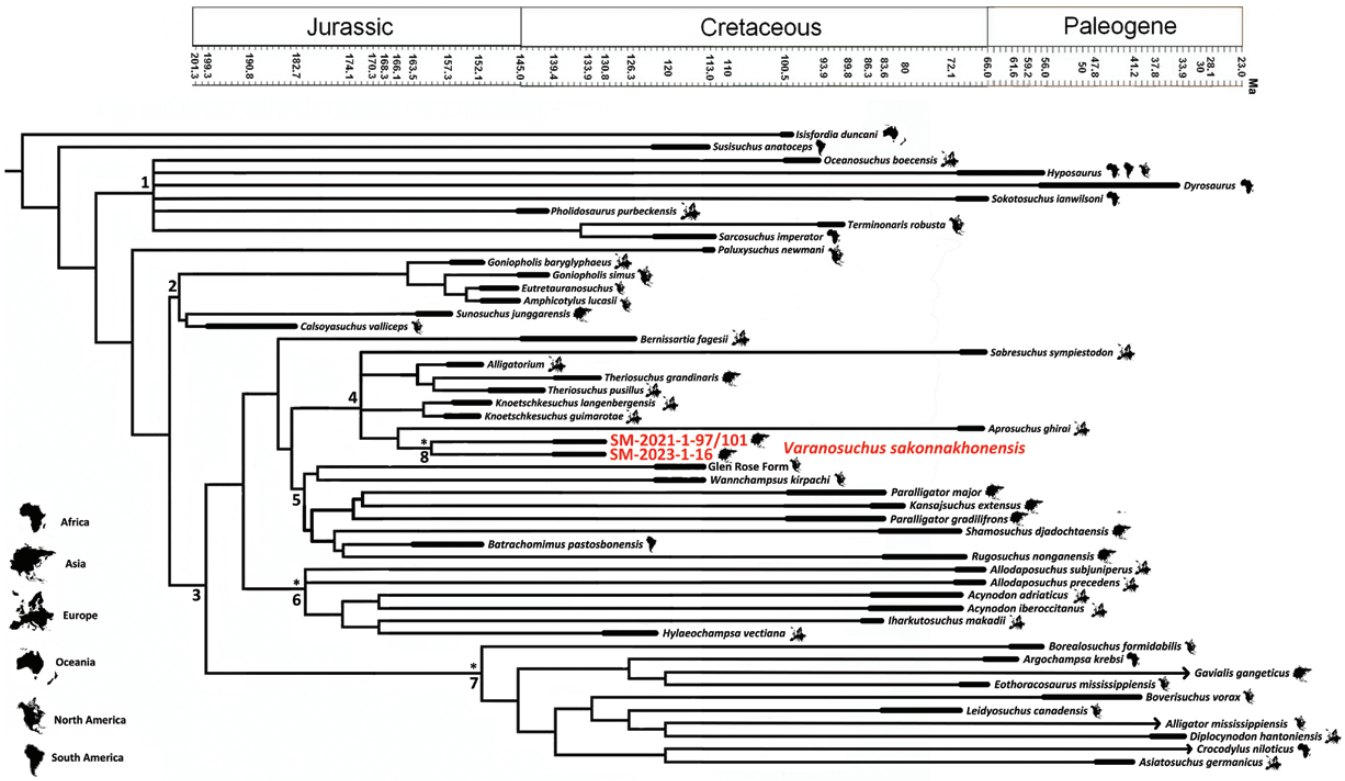

Figure 16. Time-calibrated phylogenetic tree: 1, Pholidosauridae + Dyrosauridae; 2, Goniopholididae; 3, Eusuchia; 4, Atoposauridae; 5, Paralligatoridae; 6, Hylaeochampsidae; 7, Crocodylia; 8, *Varanosuchus sakonnakhonensis*. Asterisks indicate clades displaying fully pterygoid-bound choanae.

as belonging to the genus *Sunosuchus* Young, 1948 or could be conspecific with *Siamosuchus* (Lauprasert 2004; Lauprasert *et al.* 2007, de Andrade *et al.* 2011, Puértolas-Pascual *et al.* 2015). This taxon is diagnosed on a fragment of dentary, by the following characters: dentary symphysis reaching the level of the sixth alveoli (i.e. five alveoli completely included); no marked angulation of the lower tooth row in its anterior part; no strong outward projection of the lateral rims of the third and fourth dentary alveoli; an alveolar edge strongly undulated in lateral view (Fig. 17). Although the specimen diagnosing '*Goniopholis*' *phuwiangensis* is larger than the new specimens from Phu Sung, all those characters are also shared by *SM-2021-1-97/101*. However, we argue that those characters are also identified in other neosuchians: for example, in *Goniopholis baryglyphaeus* Schwarz, 2003, the dentary referred to Goniopholididae (AR-1-3423) by Buscalioni *et al.* (2013), or *Leidyosuchus* sp. (Farke *et al.* 2014). As such, they are not truly diagnostic, and we thus consider '*Goniopholis*' *phuwiangensis* as a *nomen dubium*. The holotype of '*Goniopholis*' *phuwiangensis* could instead be referred to *Varanosuchus sakonnakhonensis*, but given its incompleteness, we would rather wait for further material to assess its belonging.

Comparisons with other closely related neosuchians

SM-2023-1-16 and *SM-2021-1-97/101* are distinguished from *Theriosuchus pusillus* Owen, 1878 because the nasal does not expand abruptly mediolaterally, the minimum infratemporal width is less than one-third of the total width of the cranial table, and the choana does not bear a septum (Tennant *et al.* 2016). Furthermore, in *SM-2021-1-97/101*, the splenial is not inset posterodorsally from the ventral surface of the mandible, the specimen does not show low-crowned teeth, the first caudal vertebra is not biconvex, and the dorsal osteoderms are not squared, which are further evidence that this specimen cannot be attributed to *T. pusillus* (Tennant *et al.* 2016).

The three specimens do not belong to *Sabresuchus ibericus* Brinkmann, 1989 because the palatal surface of the maxilla is unornamented and the tooth crowns do not have denticulate carinae (Brinkmann 1989, 1992, Tennant *et al.* 2016). Furthermore, *SM-2021-1-97/101* has eight alveoli completely involved in the mandibular symphysis, its dentary teeth are separated, the occlusal dentary surface is not compressed, and the fifth maxillary tooth is not enlarged, which are further arguments to distinguish this specimen from *Sabresuchus ibericus* (Tennant *et al.* 2016).

Finally, the three specimens are distinct from *Sabresuchus sympiestodon* Martin *et al.*, 2010 because the tooth enamel bears striations on the labial and lingual surfaces (Martin *et al.* 2010, 2014b, Tennant *et al.* 2016). *SM-2021-1-97/101* does not have a diastema between the seventh and the eighth dentary alveoli (Tennant *et al.* 2016). Furthermore, *Sabresuchus sympiestodon* has a poorly developed posterolateral process of the squamosal that projects horizontally at the same level of the skull, is narrow and unsculpted. This is not the case in *SM-2021-1-97/101* and SM-2023-1-16. The pterygoids project anteriorly at the pterygoid–palatine contact in *Sabresuchus sympiestodon*, whereas they do not in *SM-2021-1-97/101* and SM-2023-1-16; there is no depression on the posterolateral surface of the maxilla in *Sabresuchus sympiestodon*, whereas there is in *SM-2021-1-97/101* and SM-2023-1-16; the lateral margins of the frontal are flush with the skull surface in *Sabresuchus sympiestodon*, whereas they are elevated in *SM-2021-1-97/101* and SM-2023-1-16; and there is one straight to convex wave of enlarged maxillary teeth in *Sabresuchus sympiestodon*, whereas there are two sinusoidal ones in *SM-2021-1-97/101* and SM-2023-1-16. Finally, the antorbital fenestra in SM-2023-1-16 is present, whereas it is absent in *Sabresuchus sympiestodon*.

SM-2023-1-16 and *SM-2021-1-97/101* are also not attributable to Atoposauridae *sensu* Tennant *et al.* (2016), i.e. *Alligatorium* Gervais, 1871, *Alligatorellus* Gervais, 1871 and *Atoposaurus* von Meyer, 1850. For example, *Alligatorium meyeri* Jourdan, 1862 has lateral margins of the nasals that are parallel, and the lacrimal connects with the jugal (Tennant *et al.* 2016); *Atoposaurus* has unsculpted dorsal bones of the cranial table and the snout (Tennant *et al.* 2016); and *Alligatorellus* has an unopened supratemporal fenestra, a frontal thinner mediolaterally between the orbits than the nasals and with a broad anterior process, a squamosal extending to the posterior margin of the orbit, and a supraoccipital excluded from the skull roof (Tennant and Mannion 2014, Tennant *et al.* 2016). Furthermore, in *SM-2021-1-97/101*, there is no contact between the jugal and the lacrimal, there is no external mandibular fenestra, and the edges of the osteoderms are sculpted such that it is distinct from *Alligatorium meyeri*. There are osteoderms, meaning that it cannot be attributed to *Atoposaurus*. Moreover, the external surface of the mandible is sculpted, and the dorsal osteoderms do not have a lateral ridge, meaning that it is different from *Alligatorellus*.

Montsecosuchus deperiti can also be excluded because this taxon has an intertemporal width greater than its interorbital width (which is also the case for *Alligatorium paintenense* Kuhn, 1961), a very mediolaterally narrow skull, and a flat and ungrooved squamosal–parietal suture. *SM-2021-1-97/101* has a paddle-shaped retroarticular process, only two sacral vertebrae, and imbricated rectangular-shaped dorsal osteoderms, which are further elements to distinguish it from *Montsecosuchus depereti* (Tennant *et al.* 2016).

Brillanceausuchus babouriensis is also different because it has supratemporal fenestrae that are longer than the orbits, an abruptly widening nasal with sinusoidal lateral margins, a flat frontal dorsal surface, and parietal–postorbital suture visible in dorsal view (Tennant *et al.* 2016). In *SM-2021-1-97/101*, the posterolateral process of the squamosal is not depressed from the skull table, the retroarticular process is paddle shaped, and the dorsal osteoderms are rectangular, which are further arguments to distinguish it from *Brillanceausuchus babouriensis* (Tennant *et al.* 2016).

Knoetschkesuchus Schwarz *et al.*, 2017 is also different from these specimens because the minimum intertemporal width is one-third of the total width of the cranial table, the jugal bar beneath the infratemporal fenestra is flattened, the choanal groove is undivided, and the lateral margins of the frontal are elevated (Schwarz *et al.* 2017). Furthermore, *SM-2021-1-97/101* does not have an external mandibular fenestra, and the premaxilla–maxilla suture in palatal view is straight.

Another recently described taxon is *Aprosuchus ghirai* Venczel & Codrea, 2019. This taxon is diagnosed by having a W-shaped frontal–nasal suture and a heterodont dentition of at least four tooth morphotypes (pseudocaniniforms, pseudoziphodont

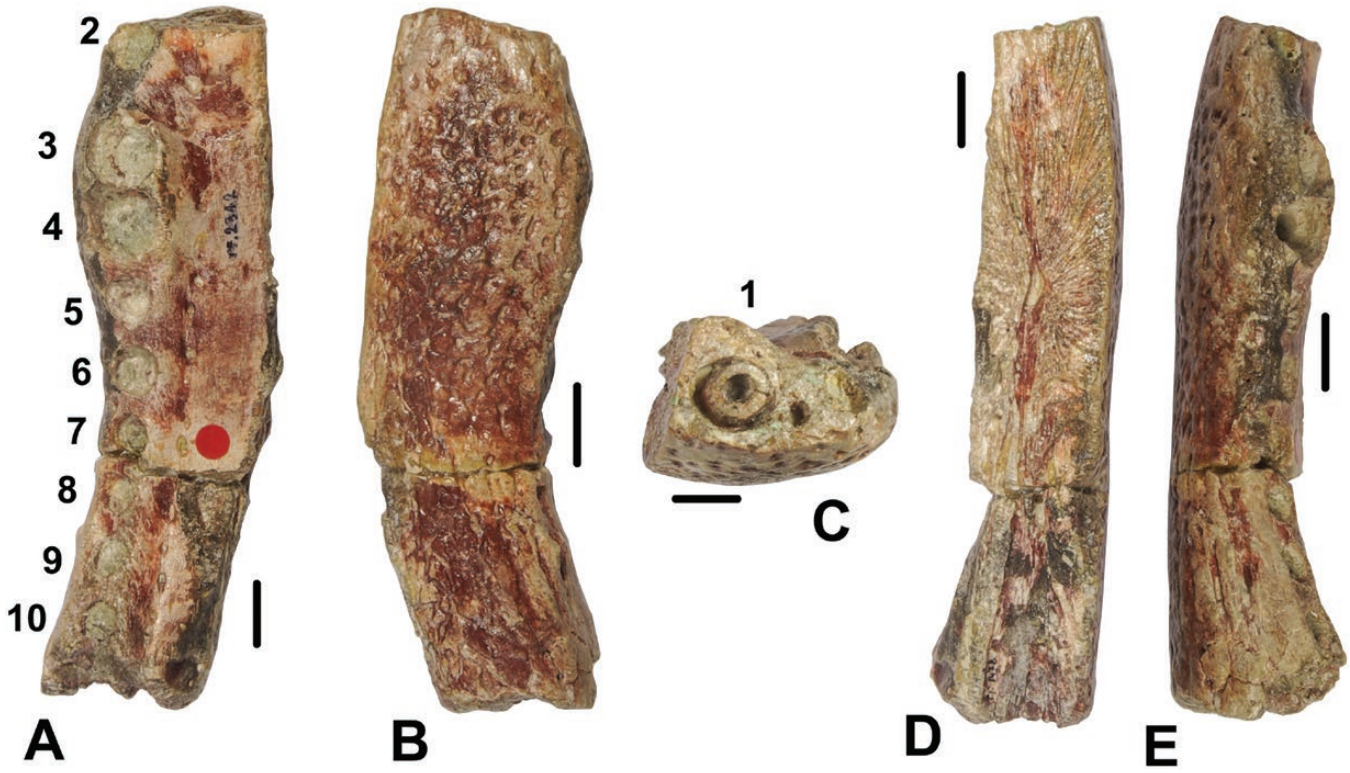

Figure 17. '*Goniopholis*' *phuwiangensis* (DMR THF 2558 1 00177) in dorsal (A), ventral (B), anterior (C), medial (D), and lateral (E) views. Numbers indicate dentary alveoli numbers. Scale bars: 1 cm.

lanceolate, ziphodont lanceolate, and 'low-crowned'). SM-2023-1-16 and *SM-2021-1-97/101* can be distinguished from this taxon because the frontal invades the nasals anteriorly, and they do not show the four tooth morphotypes. Furthermore, the quadrate, the squamosal, and the otoccipital do not meet to enclose the cranioquadrate passage in both specimens, whereas they do in *Aprosuchus*; the dorsal part of the postorbital has an anterolaterally facing edge in both specimens, whereas this bone bears only an anterior and a lateral edge in *Aprosuchus*; the quadrate has no fenestrae in both specimens, whereas it does in *Aprosuchus*; the maxillary toothrow has two waves of enlarged teeth in both specimens, whereas there is only one in *Aprosuchus*; the quadratojugal ornamentation is absent in both specimens, whereas it exists in *Aprosuchus*; the outer surface of the squamosal laterodorsally oriented is reduced and sculpted in both specimens, whereas it is reduced and unsculpted in *Aprosuchus*; and there is a depression on the posterolateral surface of the maxilla in both specimens, whereas it is absent in *Aprosuchus*.

Some taxa included in Paralligatoridae also have this altirostral morphology, but the specimens described here do not belong to this family (*sensu* Rummy *et al.* 2022) because they have at least two waves of enlargement of the maxilla and no orbitonasal sulcus on the maxilla. *SM-2021-1-97/101* also has a poorly developed quadrate intercondylar groove, whereas it is developed ventrally in paralligatorids where the condition is known; paralligatorids also possess a sharp ridge on the lateral surface of the angular and a foramen located on the premaxilla–maxilla suture near the alveolar border on the palate, whereas those features are absent in *SM-2021-1-97/101*.

More specifically, *SM-2021-1-97/101* and SM-2023-1-16 have no longitudinal ridge and no depression on the lateral surface of the jugal below the infratemporal fenestra, whereas *Shamosuchus djadochtaensis* Mook, 1924 does; the supraoccipital is exposed in the skull roof in those two specimens, whereas it is not in *Shamosuchus djadochtaensis*; the jugal anterior part is as broad as the posterior part in those two specimens, whereas it is twice as broad in *Shamosuchus djadochtaensis*; the first enlarged maxillary tooth is the fourth or the fifth one in *SM-2021-1-97/101* and SM-2023-1-16, whereas it is the second or the third one in *Shamosuchus djadochtaensis*; the squamosal posterior half has dorsal and ventral rims that are thin or parallel sided in those two specimens, whereas they are flared posteriorly in *Shamosuchus djadochtaensis*; and the anterior edge of the choanae is situated near the posterior edge of the suborbital fenestrae in *SM-2021-1-97/101* and SM-2023-1-16, whereas it is situated more anteriorly in *Shamosuchus djadochtaensis*. *SM-2021-1-97/101* also has amphicoelous cervical and dorsal vertebrae; the largest maxillary tooth is the third one; and there is a ventrally opened notch on the ventral edge of the rostrum at the premaxilla–maxilla contact, hence it can be distinguished further from *Shamosuchus djadochtaensis* (Turner 2015).

In *SM-2021-1-97/101* and SM-2023-1-16, the squamosal does not extend to the orbit in lateral view, the choanal groove is undivided, and the maxilla does not extend posteriorly in the palatines, which allow those specimens to be separated from *Paralligator* Konzhukova, 1954 (Turner 2015).

SM-2021-1-97/101 and SM-2023-1-16 can be distinguished further from *Batrachomimus pastobonensis* Montefeltro *et al.*, 2013 because these specimens do not have scalloped lateral

margins of the rostrum, do not have a long posterodorsal premaxillary process, have sculptured posterior parts of the maxilla, do not have a laterally expanded posterior part of the nasals, have palatines that are anteriorly rounded in the contact with the maxillae, and do not have a constricted choanal septum that is constricted and hourglass shaped and that extends anteriorly in the palatine (Montefeltro *et al.* 2013). *SM-2021-1-97/101* also has the jugal portion of the postorbital bar that is flush with the lateral surface of the jugal (Montefeltro *et al.* 2013).

The three specimens from Phu Sung also differ from *Rugosuchus nonganensis* Wu *et al.*, 2001 because the median ridge of the frontal continues towards the posterior end of the bone, and the median ridge of the parietal extends to the anterior end of the bone in the Phu Sung specimens (Wu *et al.* 2001). Furthermore, *SM-2021-1-97/101* and SM-2023-1-16 do not have fossae on the dorsal surface of the maxilla, and the nasals are paired and do not contact the lacrimals (Wu *et al.* 2001). Finally, in *SM-2021-1-97/101*, the angular has a gently arched dorsally posteroventral margin of the angular, whereas it is strongly arched dorsally in *Rugosuchus nonganensis*.

Wannchampsus kirpachi Adams, 2014 can also be excluded because the three specimens have the ventral rim of the earflap groove that is not laterally expanded into a sloping shelf (Adams 2014). *SM-2021-1-97/101* and SM-2023-1-16 do not have an enlarged third maxillary tooth, have a parieto-postorbital suture that is absent from the dorsal surface of the skull roof and supratemporal fossa, in addition to tooth margin carinae without crenulation, and have an internal choana bordered exclusively by the pterygoids. *SM-2021-1-97/101* does not have procoelous vertebrae and possesses an anterior dentary tooth opposite to the premaxilla–maxilla contact that is no more than the length of the other dentary teeth.

The recently described *Tarsomordeo winkleri* (Adams 2019) is different from SM-2023-1-16 because the humeral head is not semi-circular. Furthermore, we also noticed that this taxon is unfortunately undistinguishable from other close forms of the Cretaceous of North America, such as *Pachycheilosuchus trinquei* (Rogers 2003) or *Wannchampsus kirpachi* (Adams 2014); therefore, we would also cast doubt on the taxonomic status of this taxon.

Scolomastax sahlsteini (Noto *et al.* 2020) is also different from *SM-2021-1-97/101* because this taxon has a dorsal expansion on the anterodorsal part of its surangular, while *Yanjisuchus longshanensis* (Rummy *et al.* 2022) has a wedge-shaped elevation on the anterior part of the frontal, interorbital ridges with a groove in the interorbital region, and an anteroposteriorly directed ridge on the jugal that distinguish this taxon from *SM-2021-1-97/101* and SM-2023-1-16. *SM-2021-1-97/101* is further distinguished from *Yanjisuchus* because it does not have a diastema posterior to the fourth dentary tooth.

Finally, *Kansajsuchus extensus* (Kuzmin *et al.* 2019) is different from *SM-2021-1-97/101* and SM-2023-1-16 because the posterodorsal process of the premaxilla is longer, and this bone bears enlarged neurovascular foramina on its ventral surface; the nasals are separated from the external nares, contact the lacrimals, and ornamentation is absent on the alveolar margins; there are transverse crests with a dorsal groove in the interorbital region; there is a longitudinal ridge on the lateral surface of the jugal, and its anterior part is as broad as its posterior part; the supratemporal fenestrae are mediolaterally enlarged; the supraoccipital forms the dorsal edge of the foramen magnum; and the basioccipital has large pendulous tubera, with a plate below the occipital condyle that has no midline crest. In *SM-2021-1-97/101*, the enlarged maxillary alveoli are the third and the fourth, whereas they are the fourth and fifth in *Kansajsuchus*; the prefrontal is longer than the lacrimal; the palatal parts of the premaxillae meet posteriorly along the contact with the maxilla; the posterior edge of the quadrate is narrow dorsal to the otoccipital contact and strongly concave; the premaxilla–maxilla suture in palatal view is straight; and the dentary part of the mandibular symphysis completely involves five alveoli, whereas it completely involves seven to eight in *Kansajsuchus*. In SM-2023-1-16, the lateral lamina of the squamosal does not cover most of the lateral surface of the postorbital, and the otoccipital does not have a large ventrolateral part ventral to the paroccipital process, as it does in *Kansajusuchus*.

Comparisons with other small altirostral taxa

Other small altirostral forms also include *Araripesuchus* Price, 1959. However, the specimens from Phu Sung do not belong to this genus because: the parieto-postorbital suture is absent from the dorsal surface of the skull roof and the supratemporal fossa; the quadrate major axis is directed posteroventrally; the anterior edge of the internal choanae is situated near the posterior edge of the suborbital fenestra; the tooth margin carinae are not crenulated; and there are no large and aligned neurovascular foramina on the lateral maxillary surface. In *SM-2021-1-97/101*, the retroarticular process is posteriorly elongated, triangular, and facing dorsally; the postorbital process of the jugal is situated in the middle of the bone; the dentary symphysis is U-shaped, smoothly curving anteriorly in ventral view; the dorsal edge of the dentary is sinusoidal, with two concave waves; the cheek teeth are not constricted at the base of the crown; the maxillary teeth are set in isolated alveoli; and the insertion area for the muscle pterygoideus posterior does not extend onto the lateral surface of the angular. *SM-2021-1-97/101* also does not have an external mandibular fenestra, whereas the specimens assigned to *Araripesuchus* do (Ortega *et al.* 2000, Turner 2006, Dumont *et al.* 2020).

More specifically, the dorsal surface of the postorbital does not have a vascular opening, the anteromedial margins of the palatine are not parallel and they do not have parachoanal fossae, the posterior margin of the internal choanae is situated anteriorly on the pterygoids, and, in *SM-2021-1-97/101*, the lateral surface of the anterior region of the surangular and the posterior region of the dentary do not bear a longitudinal depression, and the jugal portion of the postorbital bar is medially displaced and separated from the lateral surface of the jugal [compared with *Araripesuchus buitreraensis* Pol & Apesteguía, 2005 (Dumont *et al.* 2020)].

In *SM-2021-1-97/101* and SM-2023-1-16, there are no paired ridges located medially on the ventral surface of the basisphenoid; the 10th dentary tooth is not hypertrophied in *SM-2021-1-97/101*, there is no postorbital–ectopterygoid contact, and there are no palpebrals (compared with *Araripesuchus tsangatsangana* Turner, 2006).

The parietal width is less than one-third of skull width in all specimens; the ventral edge of the maxilla is sinusoidal in lateral view in *SM-2021-1-97/101* and SM-2023-1-16; and, in *SM-2021-1-97/101*, the postorbital bar is not flush with the lateral surface of the jugal (compared with *Araripesuchus patagonicus* Ortega *et al.*, 2000).

The supratemporal fenestrae are not round, the posterior margin of the skull table is not scalloped with a median process in all specimens, and in *SM-2021-1-97/101*, there is no foramen located on the premaxilla–maxilla suture near the alveolar border [compared with *Araripesuchus wegeneri* Buffetaut, 1981 (Sereno and Larsson 2009)].

AQ19

The three specimens from Phu Sung belong to the same taxon

The phylogenetic results highlight that *SM-2021-1-97/101* and SM-2023-1-16 share six characters (see the '*Phylogenetic analyses*' subsection of the Results). Among those, SM-2023-1-17 shares with *SM-2021-1-97/101* and SM-2023-1-16 an outer surface of the squamosal laterodorsally oriented, reduced, and sculpted. Furthermore, SM-2023-1-17 also shares with *SM-2021-1-97/101* and SM-2023-1-16 an intertemporal width less than one-third of the skull width, open and ovoid supratemporal fenestrae, a supraoccipital exposed on the skull roof, a parietal width less than one-third of the skull width, and the posterior margin of the skull that is not scalloped with a median process, a parietal–postorbital suture not visible in dorsal view, and the lateral margins of the squamosal and postorbital that are not concave in dorsal view. *SM-2021-1-97/101* and SM-2023-1-17 both have a parietal surface depressed compared with the one of the squamosals, and the parietal–squamosal suture is raised and grooved. As a result, the three specimens from Phu Sung can be attributed with confidence to the same taxon.

Furthermore, all the differences observed in the description between the three specimens are part of ontogenetic variations, as highlighted in Supporting Information, Supplementary Material S8 using extant brevirostrine ontogenetic series. The associated phylogenetic characters (i.e. characters 310, 314, and 315) should thus be excluded from the character taxon matrix, because they capture ontogenetic rather than phylogenetic variation. When we apply those settings, the topology obtained does differ from the one in Figure 16, with the appearance of a polytomy between all goniopholids, and between members of Crocodylia, Hylaeochampsidae, and the clade comprising Atoposauridae *sensu* Schwarz *et al.* (2017) and Paralligatoridae *sensu* Rummy *et al.* (2022) (see also Supporting Information, Supplementary Material S6), hinting at the relative fragility of our analyses. However, the intrarelationships of the members of those two last clades do not change much, with the only difference being that in Paralligatoridae *sensu* Rummy *et al.* (2022), *Paralligator* and *Kansajsuchus* form a polytomy.

The neosuchian–eusuchian transition and the difficulty of diagnosing Atoposauridae and Eusuchia

We retrieve Atoposauridae *sensu* Schwarz *et al.* (2017) as a monophyletic group. This is contrary to what was found by Tennant *et al.* (2016) and would now include 'putative atoposaurids', such as *Theriosuchus*, *Knoetschkesuchus*, and *Sabresuchus*, in addition to *Aprosuchus ghirai* and *Varanosuchus sakonnakhonensis*, the new taxon described here. However, the intrarelationships of atoposaurids remain difficult to interpret. Although the different genera would appear to be monophyletic (Fig. 16) and are retrieved as such once phylogenetic characters that capture ontogenetic variation are excluded (Supporting Information, Supplementary Material S6), their interrelationships are not well resolved.

Paralligatoridae *sensu* Rummy *et al.* (2022) is here also retrieved in its entirety as a monophyletic group and as a sister taxon to Atoposauridae (Fig. 16). This close relationship, which had already been highlighted in other studies (Turner 2015, Turner and Pritchard 2015, Schwarz *et al.* 2017, Leite and Fortier 2018, Kuzmin *et al.* 2019, Venczel and Codrea 2019, Noto *et al.* 2020) is here strengthened with the addition of *Varanosuchus sakonnakhonensis*. The Glen Rose Form and *Wannchampsus* are retrieved as a sister taxon to all other paralligatorids, as in the studies by Adams (2014), Kuzmin *et al.* (2019), Noto *et al.* (2020), and Rummy *et al.* (2022), which confirms the very close relationship of the two operational taxonomic units and warrants a complete description and reassessment of USNM 22039. Furthermore, *Batrachomimus pastosbonensis* also warrants a complete reassessment, because it might instead be a notosuchian (Hester *et al.* 2016). However, if it is truly a paralligatorid, that implies a lack of the fossil record of this clade for >20 Myr.

AQ20

Furthermore, we propose a topology where Eusuchia includes Crocodylia, Atoposauridae, Paralligatoridae, and Hylaeochampsidae, as in the studies by Turner (2015), Schwarz *et al.* (2017), and Venczel and Codrea (2019). Susisuchidae, in contrast, is retrieved in a basal position in Neosuchia, as in work of Turner and Pritchard (2015) and Venczel and Codrea (2019). This is not that surprising, because the character taxon matrix we used here is derived mainly from this last study; however, other studies have retrieved those taxa as belonging to Eusuchia (Leite and Fortier 2018, Martin *et al.* 2020). Here, they are distinguished from Eusuchia partly because of characters that are still debated (choanal region and shape of centra; Salisbury *et al.* 2006, Turner and Prichard 2015, Leite and Fortier 2018, Montefeltro *et al.* 2019); therefore, the input of CT scan techniques on those specimens would certainly shed some light on the relationships of this family.

Our phylogenetic hypothesis thus implies a definition of Eusuchia relying on characters from the choanal, cervical, dermal shield, and supraoccipital region (see the '*Phylogenetic analyses*' subsection of the Results). Unfortunately, those characters are either reversed in subsequent clades or absent in some fossil forms, which is why we would not qualify them as truly robust for defining Eusuchia. Nonetheless, one thing is for certain: we confirm here that some of the characters historically assigned to Eusuchia (pterygoid-bound choanae and sagittal segmentation of the dorsal shield) are no longer valid with the current knowledge on ontogenetic variations and fossil forms. A striking example is that *Varanosuchus sakonnakhonensis* (depending on the status of *Brillanceausuchus babouriensis*; Michard *et al.* 1990, Tennant *et al.* 2016) is now the only definitive known atoposaurid that has fully pterygoid-bound choanae, which can be interpreted most parsimoniously as a convergence between this taxon, Hylaeochampsidae, and Crocodylia and not an apomorphy of Eusuchia, occurring two to three times independently in Eusuchia (Fig. 16). Tennant *et*

al. (2016) proposed that rather than palatine- and pterygoid-bound choanae deriving in fully pterygoid-bound choanae, the 'primitive' condition would be an anterior position of the choanae (retrieved in protosuchians, for example; Wu *et al.* 1996a) and the choanae migrating posteriorly in derived forms, reaching posteriorly to the posterior margin of the suborbital fenestrae in Hylaeochampsidae and Crocodylia (Clark and Norell 1992, Martin 2007, Delfino *et al.* 2008a, b, Ősi 2008, Martin *et al.* 2016b). Although it is correct that posteriorly placed choanae (i.e. posteriorly to the posterior margin of the suborbital fenestra) occur only in these two clades, they do not form a monophyletic group in our main analysis (Fig. 16). However, once characters depicting ontogenetic variations are removed (Supporting Information, Supplementary Material S6), hylaeochampsids cluster with crocodylians, which makes their relationships unresolved; therefore, a definite answer cannot be reached at present. A deeper sampling and knowledge of fossil forms around the neosuchian–eusuchian transition will probably permit clearer view on this matter.

The palaeoecology of atoposaurids

Although not much is known about the ecology of atoposaurids, recent studies hint at a possible terrestrial lifestyle, partly because of their very poor stratigraphic occurrences (Schwarz and Salisbury 2005) compatible with a terrestrial fossil record, in addition to their forward-facing nares (Martin *et al.* 2014b). Here, we put forward further conflicting arguments regarding this hypothesis. It has been assessed that altirostral morphology and head posture are linked directly to a terrestrial rather than semi-aquatic lifestyle, because of the implied position of the nares and binocular vision (Stevens 2006, Marinho *et al.* 2013, Pochat-Cottilloux *et al.* 2022). *Varanosuchus sakonnakhonensis* has an altirostral snout (like other atoposaurids; Tennant *et al.* 2016) and could exhibit those behaviours, making it suitable for a terrestrial lifestyle. This would, of course, be reinforced when looking at the neuroanatomy of such specimens, which, to our knowledge, remains to be done.

Furthermore, Pochat-Cottilloux *et al.* (2023b) recently proposed, building on observations by Clarac *et al.* (2018) on thermoregulatory mechanisms, that osteoderm ornamentation could be linked with lifestyle. Taxa exhibiting osteoderm ornamentation benefit of enhanced vascularization because this feature contributes to heat absorption and is thus much more needed in aquatic environments, where the physical properties are different from those on land (Schmidt-Nielsen 1997, Vogel 2005). *Varanosuchus sakonnakhonensis*, like other atoposaurids (Tennant *et al.* 2016), does have ornamented osteoderms, which could indicate semi-aquatic affinities.

The postcranial anatomy of *Varanosuchus* is remarkably well preserved and allows estimation of its posture. Terrestriality is linked with a parasagittal posture (Parrish 1987): here, *Varanosuchus* has elongated and relatively straight limb elements (Figs 9, 11C, 13C) corresponding to an erect posture (Colbert and Mook 1951, Pol *et al.* 2012, Godoy *et al.* 2016). However, using the ratio between the humerus midshaft width and long-axis length (Turner 2006, Adams 2019), we obtain a value of 0.10, which is exactly the value separating morphologies considered as 'gracile' (i.e. linked with a terrestrial lifestyle) from those considered as 'robust' (i.e. linked with a semi-aquatic/aquatic lifestyle); therefore, it is difficult to draw a conclusion regarding the posture of the organism by looking at the data provided by this bone. We thus infer a relatively erect posture for *Varanosuchus* (Fig. 18).

The various proxies for the palaeoecology of *Varanosuchus sakonnakhonensis*, and for atoposaurids in general, yield conflicting results. However, it is also possible to hypothesize a terrestrial lifestyle but with semi-aquatic affinities for those forms, as is seen today in some extant species of lepidosaurs (Mebert 2011, Chan *et al.* 2020), which would be the most probable explanation for the observations we make here. Finally, given how little evidence we have currently, the palaeoecology of paralligatorids remains an open question.

The palaeobiogeography of paralligatorids compared with atoposaurids

Although they would seem to be very close phylogenetically, definite atoposaurid and paralligatorid occurrences have different palaeogeographical and stratigraphic ranges (Fig. 16). Atoposaurids have a Laurasian distribution, whereas paralligatorids are known only in Asia and in North America (maybe also in South America, but see above).

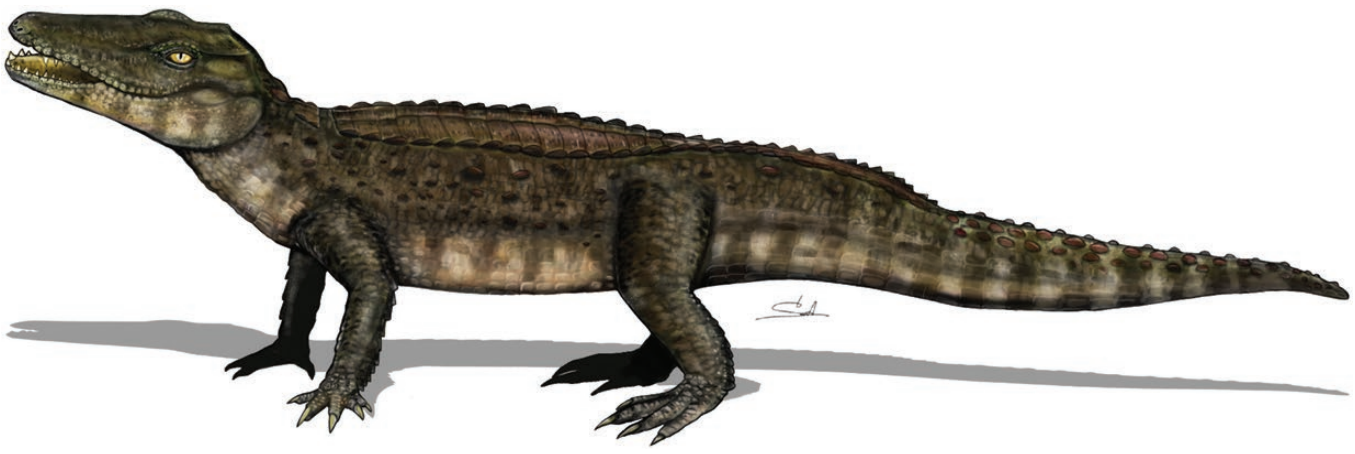

Figure 18. Reconstruction of *Varanosuchus sakonnakhonensis* in its living posture.

In terms of stratigraphic range, atoposaurids are present in Late Jurassic to Early Cretaceous strata, with *Sabresuchus sympiestodon* and *Aprosuchus ghirai* being the only representatives of this family in the Late Cretaceous, implying lack of a fossil record for >50 Myr. This huge stratigraphic gap could be filled when looking at specimens that may be attributed to Atoposauridae in the Cenomanian (Vullo and Néraudeau 2008) and Campanian–Maastrichtian of France (Martin and Buffetaut 2005, Martin *et al.* 2014b), Middle Cretaceous of the USA (Winkler *et al.* 1990, Cifelli *et al.* 1999, Eaton *et al.* 1999, Fiorillo 1999, Garrison *et al.* 2007, Oreska *et al.* 2013, Foster 2018), and Aptian–Albian of China (Wu *et al.* 1996b, Mo *et al.* 2016). Finally, the referral of some specimens from the Eocene of Yemen to Atoposauridae (Stevens *et al.* 2013) is very surprising and also warrants further investigation. In contrast, except for *Batrachomimus pastosbonensis* (for which a reassessment might be necessary; Hester *et al.* 2016), paralligators are known from the Middle to Late Cretaceous (Fig. 16). One interesting thing to notice is that the two families have never been retrieved at the same time and the same place, which could be because the competition for resources between these two groups of very similar organisms would have been too important for them to cohabit, hinting at a similar ecology, or could also be a case of collection bias.

CONCLUSION

We describe here three new specimens from the Early Cretaceous Phu Sung locality (Sao Khua Formation, Thailand) that we refer to *Varanosuchus sakonnakhonensis*. Using CT scan data, we can provide an in-depth description, in addition to a comparison with other close fossil forms. Although we notice some ontogenetic variations, *Varanosuchus sakonnakhonensis* is diagnosed by an altirostral morphology, a dorsal part of the postorbital with an anterolaterally facing edge, a depression on the posterolateral surface of the maxilla, and fully pterygoid-bound choanae, among other traits.

A phylogenetic analysis confirms that this new taxon belongs to Atoposauridae *sensu* Schwarz *et al.* (2017), with a close relationship to *Aprosuchus ghirai* from the Maastrichtian of Romania (Venczel and Codrea 2019). We also manage to distinguish this taxon from *Theriosuchus grandinaris* (Lauprasert *et al.* 2011) from the same age also in Thailand. Paralligatoridae *sensu* Rummy *et al.* (2022) are retrieved as the sister clade to Atoposauridae, forming Eusuchia with Hylaeochampsidae and Crocodylia, while susisuchids are found as basal neosuchians; characters historically assigned to Eusuchia, such as fully pterygoid-bound choanae, are no longer valid. However, a robust definition of Eusuchia must still be provided.

Finally, the altirostral snout morphology and osteoderm ornamentation observed here in *Varanosuchus sakonnakhonensis* (and other atoposaurids) would match the hypothesis for those taxa of a terrestrial lifestyle with semi-aquatic affinities. Further studies are needed to confirm this, for example using neuroanatomical or geochemical proxies.

SUPPLEMENTARY DATA

Supplementary data is available at *Zoological Journal of the Linnean Society* online.

ACKNOWLEDGEMENTS

We thank Céline Salaviale, Vincent Perrier, and Jeanne Rolland (Univ Lyon 1) for technical support, in addition to Didier Berthet (Musée des Confluences de Lyon), Lawrence Witmer (Ohio University), Thomas van der Kamp and Marcus Zuber (Staatliche Museum für Naturkunde Karlsruhe), Timothy Rowe (University of Texas), Blandine Bartschi (Univ Lyon 1), Sébastien Bruaux (Royal Belgian Institute of Natural Sciences), Silke Schweiger and Viola Winkler (Natural History Museum Vienna), Medhi Mouana and Anne-Lise Charruault (University of Montpellier), Cody Thompson (University of Michigan), David Blackburn (Florida Museum of Natural History), Patrick Campbell and Susannah Maidment (Natural History Museum, UK), and Christophe Borrely (Muséum d'Histoire Naturelle de Marseille) for access to extant specimens. We would also like to thank Jeff Streicher (Natural History Museum, UK), Márton Rabi (University of Tübingen, Germany), and an anonymous reviewer for their comments that greatly improved this manuscript.

CONFLICT OF INTEREST

None declared.

FUNDING

This work was supported by the Agence Nationale de la Recherche (SEBEK project no. ANR-19-CE31-0006-01 to J.E.M.) and the International Research Group PalBioDivASE (IRN) grant of CNRS.

DATA AVAILABILITY

The data underlying this article are available in the article and in its Supporting Information.

REFERENCES

Adams TL. Small crocodyliform from the Lower Cretaceous (late Aptian) of central Texas and its systematic relationship to the evolution of Eusuchia. *Journal of Paleontology* 2014;**88**:1031–49. https://doi.org/10.1666/12-089

Adams TL. Small terrestrial crocodyliform from the Lower Cretaceous (late Aptian) of central Texas and its implications on the paleoecology of the Proctor Lake Dinosaur locality. *Journal of Vertebrate Paleontology* 2019;**39**:e1623226. https://doi.org/10.1080/02724634.2019.1623226

Benton RBJ, Clark JM. Archosaur phylogeny and the relationships of the Crocodylia. In: Benton MJ (ed.), *The Phylogeny and Classification of the Tetrapods, Vol. 1, Amphibians, Reptiles, Birds*. Oxford University Press, 1988, 295–338.

Brinkmann W. Vorläufige Mitteilung über die Krokodilier-Faunen aus dem Ober-Jura (Kimmeridgium) der Kohlegrube Guimarota, bei Leiria (Portugal) und der Unter-Kreide (Barremium) von Una (Provinz Cuenca, Spanien). *Documenta Naturae* 1989;**56**:1–28.

Brinkmann W. Die Krokodilier-Fauna aus der Unter-Kreide (Ober-Barremium) von Una (Provinz Cuenca, Spanien). *Berliner Geowissenschaftliche Abhandlungen* 1992;**5**:1–123.

Buffetaut E. Die biogeographische Geschichte der Krokodilier, mit Beschreibung einer neuen Art, *Araripesuchus wegeneri*. *Geologische Rundschau* 1981;**70**:611–24. https://doi.org/10.1007/bf01822139

Buffetaut E, Ingavat R. A new crocodilian from the Jurassic of Thailand, *Sunosuchus thailandicus* n. sp. (Mesosuchia, Goniopholididae), and the palaeogeographical history of South-East Asia in the Mesozoic. *Geobios* 1980;**13**:879–89. https://doi.org/10.1016/s0016-6995(80)80042-8

Buffetaut E, Ingavat R. *Goniopholis phuwiangensis* nov. sp., a new mesosuchian crocodile from the Mesozoic of north-eastern Thailand. *Geobios* 1983;**16**:79–91. https://doi.org/10.1016/s0016-6995(83)80048-5

Buffetaut E, Ingavat R. The lower jaw of *Sunosuchus thailandicus*, a mesosuchian crocodilian from the Jurassic of Thailand. *Palaeontology* 1984;**27**:199–206.

Buscalioni AD, Alcalá L, Espílez E *et al.* European Goniopholididae from the Early Albian Escucha Formation in Ariño (Teruel, Aragón, Spain). *Spanish Journal of Palaeontology* 2013;**28**:103–22. https://doi.org/10.7203/sjp.28.1.17835

Chan WH, Lau A, Martelli P *et al.* Spatial ecology of the introduced Chinese water dragon *Physignathus cocincinus* in Hong Kong. *Current Herpetology* 2020;**39**:55–65. https://doi.org/10.5358/hsj.39.55

Chanthasit P, Suteethorn S, Naksri W *et al.* New vertebrate fossil site from the Early Cretaceous Sao Khua Formation, Sakon Nakhon Province, Northeastern Thailand. *Open Journal of Geology* 2019;**09**:619–22. https://doi.org/10.4236/ojg.2019.910057

Cifelli RL, Nydam RL, Gardner JD *et al.* Medial Cretaceous vertebrates from the Cedar Mountain Formation, Emery County, Utah: the Mussentuchit local fauna. *Vertebrate Paleontology in Utah* 1999;**99**:219–42.

Clarac F, de Buffrénil V, Cubo J *et al.* Vascularization in ornamented osteoderms: physiological implications in ectothermy and amphibious lifestyle in the crocodylomorphs? *Anatomical Record* 2018;**301**:175–83. https://doi.org/10.1002/ar.23695

Clark JM. Phylogenetic relationships of the crocodylomorph archosaurs. Unpublished D.Phil. Thesis, University of Chicago, 1986.

Clark JM. Patterns of evolution in Mesozoic Crocodyliformes. In: Fraser NC, Sues HD (eds.), *In the Shadows of Dinosaurs: Early Mesozoic Tetrapods*. Cambridge University Press, 1994, 84–97.

Clark JM, Norell M. The Early Cretaceous crocodylomorph *Hylaeochampsa vectiana* from the Wealden of the Isle of Wight. *American Museum Novitates* 1992;**3032**:1–19.

Colbert EH, Mook CC. The ancestral crocodilian *Protosuchus*. *Bulletin of the American Museum of Natural History* 1951;**97**:143–82.

Congreve CR, Lamsdell JC. Implied weighting and its utility in palaeontological datasets: a study using modelled phylogenetic matrices. *Palaeontology* 2016;**59**:447–62. https://doi.org/10.1111/pala.12236

de Andrade MB, Edmonds R, Benton MJ *et al.* A new Berriasian species of *Goniopholis* (Mesoeucrocodylia, Neosuchia) from England, and a review of the genus. *Zoological Journal of the Linnean Society* 2011;**163**:S66–S108. https://doi.org/10.1111/j.1096-3642.2011.00709.x

Delfino M, Codrea V, Folie A *et al.* A complete skull of *Allodaposuchus precedens* Nopcsa, 1928 (Eusuchia) and a reassessment of the morphology of the taxon based on the Romanian remains. *Journal of Vertebrate Paleontology* 2008a;**28**:111–22. https://doi.org/10.1671/0272-4634(2008)28[111:acsoap]2.0.co;2

Delfino M, Martin JE, Buffetaut E. A new species of *Acynodon* (Crocodylia) from the Upper Cretaceous (Santonian–Campanian) of Villaggio del Pescatore, Italy. *Palaeontology* 2008b;**51**:1091–106. https://doi.org/10.1111/j.1475-4983.2008.00800.x

Ditbanjong P, Chanthasit P, Wongko K. Sedimentology and stratigraphy of Phu Sung fossil site of the Lower Cretaceous Sao Khua Formation, Sakon Nakhon Province, Northeastern Thailand. *Open Journal of Geology* 2019;**09**:684–7. https://doi.org/10.4236/ojg.2019.910075

Dollo L. Première note sur les crocodiliens de Bernissart. *Bulletin du Musée Royal d'Histoire Naturelle de Belgique* 1883;**2**:309–38.

Dumont MF, Bona P, Pol D *et al.* New anatomical information on *Araripesuchus buitreraensis* with implications for the systematics of Uruguaysuchidae (Crocodyliforms, Notosuchia). *Cretaceous Research* 2020;**113**:104494.

Eaton JG, Cifelli RL, Hutchison JH *et al.* Cretaceous vertebrate faunas from the Kaiparowits Plateau, south-central Utah. *Vertebrate Paleontology in Utah* 1999;**99**:345–52.

Efimov MB. New paralligatorids from the Upper Cretaceous of Mongolia. *Trudy Sovmestnoi Sovetsko-Mongol'skoi Paleontologicheskoi Ekspeditsii* 1981;**15**:26–8.

Efimov MB. Review of fossil crocodiles of Mongolia. *Trudy Sovmestnoi Sovetsko-Mongol'skoi Paleontologischeskoi Ekspeditsii* 1983;**24**:76–96.

Eijkelboom I. Postcranial remains of *Knoetschkesuchus guimarotae* (Atoposauridae, Crocodylomorpha) from the Late Jurassic of Portugal and its locomotor behaviour. Unpublished Master's thesis, Utrecht University, 2020.

Farke AA, Henn MM, Woodward SJ *et al.* *Leidyosuchus* (Crocodylia: Alligatoroidea) from the Upper Cretaceous Kaiparowits Formation (late Campanian) of Utah, USA. *PaleoBios* 2014;**30**:72–88.

Farris JS. Methods for computing Wagner trees. *Systematic Biology* 1970;**19**:83–92. https://doi.org/10.1093/sysbio/19.1.83

Fiorillo AR. Non-mammalian microvertebrate remains from the Robison Eggshell site, Cedar Mountain Formation (Lower Cretaceous), Emery County, Utah. *Vertebrate Paleontology in Utah* 1999;**99**:259–68.

Foster J. A new atoposaurid crocodylomorph from the Morrison Formation (Upper Jurassic) of Wyoming, USA. *Geology of the Intermountain West* 2018;**5**:287–95. https://doi.org/10.31711/giw.v5.pp287-295

Garrison JR, Brinkman D, Nichols DJ *et al.* A multidisciplinary study of the Lower Cretaceous Cedar Mountain Formation, Mussentuchit Wash, Utah: a determination of the paleoenvironment and paleoecology of the *Eolambia caroljonesa* dinosaur quarry. *Cretaceous Research* 2007;**28**:461–94. https://doi.org/10.1016/j.cretres.2006.07.007

Gervais P. Remarques au sujet des Reptiles provenant des calcaires lithographiques de Cirin, dans le Bugey, qui sont conservés au Musée de Lyon. *Comptes Rendus Sommaire des Seances de la Societe geologique de France* 1871;**73**:603–7.

Godoy PL, Bronzati M, Eltink E *et al.* Postcranial anatomy of *Pissarrachampsa sera* (Crocodyliformes, Baurusuchidae) from the Late Cretaceous of Brazil: insights on lifestyle and phylogenetic significance. *PeerJ* 2016;**4**:e2075. https://doi.org/10.7717/peerj.2075

Goloboff PA. Analyzing large data sets in reasonable times: solutions for composite optima. *Cladistics* 1999;**15**:415–28. https://doi.org/10.1111/j.1096-0031.1999.tb00278.x

Goloboff PA. Extended implied weighting. *Cladistics* 2014;**30**:260–72. https://doi.org/10.1111/cla.12047

Goloboff PA, Catalano SA. TNT version 15, including a full implementation of phylogenetic morphometrics. *Cladistics* 2016;**32**:221–38. https://doi.org/10.1111/cla.12160

Gomes de Souza R. Comments on the serial homology and homologues of vertebral lateral projections in Crocodylia (Eusuchia). *The Anatomical Record* 2018;**301**:1203–15.

Groh SS, Upchurch P, Barrett PM *et al.* The phylogenetic relationships of neosuchian crocodiles and their implications for the convergent evolution of the longirostrine condition. *Zoological Journal of the Linnean Society* 2020;**188**:473–506.

Hay OP. *Second Bibliography and Catalogue of the Fossil Vertebrata of North America*. Washington, DC, 1930.

Hester DA, Brochu CA, Turner AH. A re-evaluation of the crocodyliform *Batrachomimus pastosbonensis* from the Late Jurassic of Brazil: implications for neosuchian phylogeny, biogeography, and divergence timing. In: *76th Annual Meeting of the Society of Vertebrate Paleontology*, Salt Lake City, 2016.

Iordansky NN. The skull of the Crocodilia. *Biology of the Reptilia* 1973;**4**:201–62.

Jourdan C. Une communication relative à deux nouveaux fossiles trouvés dans le calcaire lithographique de Cirin. *Annales des Sciences Physiques et Naturelles de la Société d'Agriculture et d'Industrie de Lyon 3rd series* 1862;**6**:32–3.

Jouve S. A new basal tomistomine (Crocodylia, Crocodyloidea) from Issel (Middle Eocene; France): palaeobiogeography of basal tomistomines and palaeogeographic consequences. *Zoological Journal of the Linnean Society* 2016;**177**:165–82. https://doi.org/10.1111/zoj.12357

Jouve S, Iarochene M, Bouya B *et al.* A new species of *Dyrosaurus* (Crocodylomorpha, Dyrosauridae) from the early Eocene of Morocco: phylogenetic implications. *Zoological Journal of the Linnean Society* 2006;**148**:603–56.

Konzhukova ED. New fossil crocodilian from Mongolia. *Trudy Paleontologicheskogo Instituta ANSSSR* 1954;**48**:171–94.

Kubo T, Shibata M, Naksri W *et al*. The earliest record of Asian Eusuchia from the Lower Cretaceous Khok Kruat formation of northeastern Thailand. *Cretaceous Research* 2018;**82**:21–8. https://doi.org/10.1016/j.cretres.2017.05.021

Kuhn O. Die Tier-und pflanzenweit des Solnhofener Schiefers. *Geologica Bavarica* 1961;**48**.

Kuzmin IT, Skutschas PP, Boitsova EA *et al*. Revision of the large crocodyliform *Kansajsuchus* (Neosuchia) from the Late Cretaceous of Central Asia. *Zoological Journal of the Linnean Society* 2019;**185**:335–87.

Kuzmin IT, Boitsova EA, Gombolevskiy VA *et al*. Braincase anatomy of extant Crocodylia, with new insights into the development and evolution of the neurocranium in crocodylomorphs. *Journal of Anatomy* 2021;**239**:983–1038. https://doi.org/10.1111/joa.13490

Lauprasert K. Evolution and palaeoecology of crocodiles in the Mesozoic of Khorat Plateau. Unpublished PhD thesis, Chulalongkorn University, 2006.

Lauprasert K, Cuny G, Buffetaut E *et al*. *Siamosuchus phuphokensis*, a new goniopholidid from the Early Cretaceous (ante-Aptian) of northeastern Thailand. *Bulletin de la Société géologique de France* 2007;**178**:201–16. https://doi.org/10.2113/gssgfbull.178.3.201

Lauprasert K, Cuny G, Thirakhupt K *et al*. *Khoratosuchus jintasakuli* gen. et sp. nov., an advanced neosuchian crocodyliform from the Early Cretaceous (Aptian-Albian) of NE Thailand. *Geological Society, London, Special Publications* 2009;**315**:175–87. https://doi.org/10.1144/sp315.13

Lauprasert K, Laojumpon C, Saenphala W *et al*. Atoposaurid crocodyliforms from the Khorat Group of Thailand: first record of *Theriosuchus* from Southeast Asia. *Paläontologische Zeitschrift* 2011;**85**:37–47. https://doi.org/10.1007/s12542-010-0071-z

Leite KJ, Fortier DC. The palate and choanae structure of the *Susisuchus anatoceps* (Crocodyliformes, Eusuchia): phylogenetic implications. *PeerJ* 2018;**6**:e5372. https://doi.org/10.7717/peerj.5372

Marinho TDS, Iori FV, Carvalho IDS *et al*. *Gondwanasuchus scabrosus* gen. et sp. nov., a new terrestrial predatory crocodyliform (Mesoeucrocodylia: Baurusuchidae) from the Late Cretaceous Bauru Basin of Brazil. *Cretaceous Research* 2013;**44**:104–11.

Martin JE. New material of the Late Cretaceous globidontan *Acynodon iberoccitanus* (Crocodylia) from southern France. *Journal of Vertebrate Paleontology* 2007;**27**:362–72. https://doi.org/10.1671/0272-4634(2007)27[362:nmotlc]2.0.co;2

Martin JE, Buffetaut E. An overview of the Late Cretaceous crocodilian assemblage from Cruzy, southern France. *Kaupia* 2005;**14**:33–40.

Martin JE, Rabi M, Csiki Z. Survival of *Theriosuchus* (Mesoeucrocodylia: Atoposauridae) in a Late Cretaceous archipelago: a new species from the Maastrichtian of Romania. *Naturwissenschaften* 2010;**97**:845–54. https://doi.org/10.1007/s00114-010-0702-y

Martin JE, Lauprasert K, Buffetaut E *et al*. A large pholidosaurid in the Phu Kradung Formation of north-eastern Thailand. *Palaeontology* 2014a;**57**:757–69. https://doi.org/10.1111/pala.12086

Martin JE, Rabi M, Csiki-Sava Z *et al*. Cranial morphology of *Theriosuchus sympiestodon* (Mesoeucrocodylia, Atoposauridae) and the widespread occurrence of *Theriosuchus* in the Late Cretaceous of Europe. *Journal of Paleontology* 2014b;**88**:444–56. https://doi.org/10.1666/13-106

Martin JE, Raslan-Loubatié J, Mazin JM. Cranial anatomy of *Pholidosaurus purbeckensis* from the Lower Cretaceous of France and its bearing on pholidosaurid affinities. *Cretaceous Research* 2016a;**66**:43–59. https://doi.org/10.1016/j.cretres.2016.05.008

Martin JE, Delfino M, Garcia G *et al*. New specimens of *Allodaposuchus precedens* from France: intraspecific variability and the diversity of European Late Cretaceous eusuchians. *Zoological Journal of the Linnean Society* 2016b;**176**:607–31.

Martin JE, Smith T, Salaviale C *et al*. Virtual reconstruction of the skull of *Bernissartia fagesii* and current understanding of the neosuchian–eusuchian transition. *Journal of Systematic Palaeontology* 2020;**18**:1079–101. https://doi.org/10.1080/14772019.2020.1731722

Mebert K. The dice snake, *Natrix tessellata*: biology, distribution and conservation of a Palaearctic species. *Mertensiella* 2011;**18**:1–456.

Meunier LMV. Phylogeny of Pholidosauridae. Unpublished D.Phil. Thesis, McGill University, 2017.

Michard JG, De Broin F, Brunet M *et al*. Le plus ancien crocodilien néosuchien spécialisé à caractères 'eusuchiens' du continent africain (Crétacé inférieur, Cameroun). *Comptes Rendus de l'Académie des Sciences Paris* 1990;**311**:365–71.

Mo J, Buffetaut E, Tong H *et al*. Early Cretaceous vertebrates from the Xinlong Formation of Guangxi (southern China): a review. *Geological Magazine* 2016;**153**:143–59. https://doi.org/10.1017/s0016756815000394

Montefeltro FC, Larsson HC, de França MA *et al*. A new neosuchian with Asian affinities from the Jurassic of northeastern Brazil. *Naturwissenschaften* 2013;**100**:835–41. https://doi.org/10.1007/s00114-013-1083-9

Montefeltro FC, Bronzati M, Langer MC *et al*. A new specimen *of Susisuchus anatoceps* (Crocodyliformes, Neosuchia) with a non-eusuchian-type palate. *Journal of Vertebrate Paleontology* 2019;**39**:e1716240. https://doi.org/10.1080/02724634.2019.1716240

Mook CC. Notes on the postcranial skeleton in the Crocodilia. *Bulletin of the American Museum of Natural History* 1921;**44**:67–100.

Mook CC. A new crocodilian from Mongolia. *American Museum Novitates* 1924;**117**:1–5.

Nixon KC. The parsimony ratchet, a new method for rapid parsimony analysis. *Cladistics* 1999;**15**:407–14. https://doi.org/10.1111/j.1096-0031.1999.tb00277.x

Noto CR, Drumheller SK, Adams TL *et al*. An enigmatic small neosuchian crocodyliform from the Woodbine Formation of Texas. *Anatomical Record* 2020;**303**:801–12. https://doi.org/10.1002/ar.24174

Oreska MP, Carrano MT, Dzikiewicz KM. Vertebrate paleontology of the Cloverly Formation (Lower Cretaceous), I: faunal composition, biogeographic relationships, and sampling. *Journal of Vertebrate Paleontology* 2013;**33**:264–92.

Ortega F, Gasparini Z, Buscalioni AD *et al*. A new species of *Araripesuchus* (Crocodylomorpha, Mesoeucrocodylia) from the lower Cretaceous of Patagonia (Argentina). *Journal of Vertebrate Paleontology* 2000;**20**:57–76. https://doi.org/10.1671/0272-4634(2000)020[0057:ansoac]2.0.co;2

Ősi A. Cranial osteology of *Iharkutosuchus makadii*, a Late Cretaceous basal eusuchian crocodyliform from Hungary. *Neues Jahrbuch für Geologie und Paläontologie - Abhandlungen* 2008;**248**:279–99. https://doi.org/10.1127/0077-7749/2008/0248-0279

Owen R. On the fossils called 'granicones': being a contribution to the histology of the exo-skeleton in 'Reptilia'. *Journal of the Royal Microscopical Society* 1878;**1**:222–36.

Parrish JM. The origin of crocodilian locomotion. *Paleobiology* 1987;**13**:396–414. https://doi.org/10.1017/s0094837300009003

Pochat-Cottilloux Y, Martin JE, Jouve S *et al*. The neuroanatomy of *Zulmasuchus querejazus* (Crocodylomorpha, Sebecidae) and its implications for the paleoecology of sebecosuchians. *The Anatomical Record* 2022;**305**:2708–28.

Pochat-Cottilloux Y, Perrier V, Amiot R *et al*. A peirosaurid mandible from the Albian/Cenomanian (Lower Cretaceous) of Algeria and the taxonomic content of *Hamadasuchus* (Crocodylomorpha, Peirosauridae). *Papers in Palaeontology* 2023a;**9**:e1485.

Pochat-Cottilloux Y, Martin JE, Amiot R *et al*. A survey of osteoderm histology and ornamentation among Crocodylomorpha: a new proxy to infer lifestyle? *Journal of Morphology* 2023b;**284**:e21542.

Pol D, Apesteguía S. New *Araripesuchus* remains from the early Late Cretaceous (Cenomanian–Turonian) of Patagonia. *American Museum Novitates* 2005;**2005**:1–38.

Pol D, Turner AH, Norell MA. Morphology of the Late Cretaceous crocodylomorph *Shamosuchus djadochtaensis* and a discussion of neosuchian phylogeny as related to the origin of Eusuchia. *Bulletin of the American Museum of Natural History* 2009;**2009**:1–103.

Pol D, Leardi JM, Lecuona A *et al*. Postcranial anatomy of *Sebecus icaeorhinus* (Crocodyliformes, Sebecidae) from the Eocene of Patagonia. *Journal of Vertebrate Paleontology* 2012;**32**:328–54. https://doi.org/10.1080/02724634.2012.646833

Price LI. Sôbre um crocodilídeo Notossúquio do Cretácico Brasileiro. *Boletim do Departamento Nacional da Produçao Mineral, Divisao de Geologia e Mineralogia, Rio de Janeiro* 1959;**188**:7–55.

Puértolas-Pascual E, Mateus O. A three-dimensional skeleton of Goniopholididae from the Late Jurassic of Portugal: implications for the Crocodylomorpha bracing system. *Zoological Journal of the Linnean Society* 2020;**189**:521–48.

Puértolas-Pascual E, Canudo JI, Sender LM. New material from a huge specimen of *Anteophthalmosuchus* cf. *escuchae* (Goniopholididae) from the Albian of Andorra (Teruel, Spain): phylogenetic implications. *Journal of Iberian Geology* 2015;**41**:41–56.

Ristevski J, Young MT, De Andrade MB *et al*. A new species of *Anteophthalmosuchus* (Crocodylomorpha, Goniopholididae) from the Lower Cretaceous of the Isle of Wight, United Kingdom, and a review of the genus. *Cretaceous Research* 2018;**84**:340–83. https://doi.org/10.1016/j.cretres.2017.11.008

Rogers JV. *Pachycheilosuchus trinquei*, a new procoelous crocodyliform from the Lower Cretaceous (Albian) Glen Rose Formation of Texas. *Journal of Vertebrate Paleontology* 2003;**23**:128–45. https://doi.org/10.1671/0272-4634(2003)23[128:ptanpc]2.0.co;2

Romer AS. The Chañares (Argentina) Triassic reptile fauna. XIII. An early ornithosuchid pseudosuchian, *Gracilisuchus stipanicicorum*, gen. et sp. nov. *Breviora* 1972;**389**:1–24.

Rummy P, Wu XC, Clark JM *et al*. A new paralligatorid (Crocodyliformes, Neosuchia) from the mid-Cretaceous of Jilin Province, northeastern China. *Cretaceous Research* 2022;**129**:105018. https://doi.org/10.1016/j.cretres.2021.105018

Salisbury SW, Frey E. A biomechanical transformation model for the evolution of semi-spheroidal articulations between adjoining vertebral bodies in crocodilians. In: Grigg C, Seebacher F, Franklin CE (eds.), *Crocodilian Biology and Evolution*, 2001, 85–134.

Salisbury SW, Molnar RE, Frey E *et al*. The origin of modern crocodyliforms: new evidence from the Cretaceous of Australia. *Proceedings Biological Sciences* 2006;**273**:2439–48. https://doi.org/10.1098/rspb.2006.3613

Schmidt-Nielsen K. *Animal Physiology: Adaptation and Environment*. Cambridge: Cambridge University Press, 1997.

Schwarz D. A new species of *Goniopholis* from the Upper Jurassic of Portugal. *Palaeontology* 2003;**45**:185–208. https://doi.org/10.1111/1475-4983.00233

Schwarz D, Salisbury SW. A new species of *Theriosuchus* (Atoposauridae, Crocodylomorpha) from the late Jurassic (Kimmeridgian) of Guimarota, Portugal. *Geobios* 2005;**38**:779–802. https://doi.org/10.1016/j.geobios.2004.04.005

Schwarz D, Raddatz M, Wings O. *Knoetschkesuchus langenbergensis* gen. nov. sp. nov., a new atoposaurid crocodyliform from the Upper Jurassic Langenberg Quarry (Lower Saxony, northwestern Germany), and its relationships to *Theriosuchus*. *PLoS One* 2017;**12**:e0160617. https://doi.org/10.1371/journal.pone.0160617

Sereno PC, Larsson HC. Cretaceous crocodyliforms from the Sahara. *ZooKeys* 2009;**28**:1–143. https://doi.org/10.3897/zookeys.28.325

Stevens KA. Binocular vision in theropod dinosaurs. *Journal of Vertebrate Paleontology* 2006;**26**:321–30. https://doi.org/10.1671/0272-4634(2006)26[321:bvitd]2.0.co;2

Stevens NJ, Hill RV, Al-Wosabi M *et al*. A middle Eocene mesoeucrocodylian (Crocodyliformes) from the Kaninah Formation, Republic of Yemen. *Geologos* 2013;**19**:175–83. https://doi.org/10.2478/logos-2013-0010

Sweetman SC, Pedreira-Segade U, Vidovic SU. A new bernissartiid crocodyliform from the Lower Cretaceous Wessex Formation (Wealden Group, Barremian) of the Isle of Wight, southern England. *Acta Palaeontologica Polonica* 2014;**60**:257–68.

Swofford DL, Maddison WP. Reconstructing ancestral character states under Wagner parsimony. *Mathematical Biosciences* 1987;**87**:199–229. https://doi.org/10.1016/0025-5564(87)90074-5

Tennant JP, Mannion PD. Revision of the Late Jurassic crocodyliform *Alligatorellus*, and evidence for allopatric speciation driving high diversity in western European atoposaurids. *PeerJ* 2014;**2**:e599. https://doi.org/10.7717/peerj.599

Tennant JP, Mannion PD, Upchurch P. Evolutionary relationships and systematics of Atoposauridae (Crocodylomorpha: Neosuchia): implications for the rise of Eusuchia. *Zoological Journal of the Linnean Society* 2016;**177**:854–936. https://doi.org/10.1111/zoj.12400

Tucker RT, Hyland EG, Gates TA *et al*. Age, depositional history, and paleoclimatic setting of Early Cretaceous dinosaur assemblages from the Sao Khua Formation (Khorat Group), Thailand. *Palaeogeography, Palaeoclimatology, Palaeoecology* 2022;**601**:111107. https://doi.org/10.1016/j.palaeo.2022.111107

Turner AH. Osteology and phylogeny of a new species of *Araripesuchus* (Crocodyliformes: Mesoeucrocodylia) from the Late Cretaceous of Madagascar. *Historical Biology* 2006;**18**:255–369. https://doi.org/10.1080/08912960500516112

Turner AH. A review of *Shamosuchus* and *Paralligator* (Crocodyliformes, Neosuchia) from the Cretaceous of Asia. *PLoS One* 2015;**10**:e0118116. https://doi.org/10.1371/journal.pone.0118116

Turner AH, Buckley GA. *Mahajangasuchus insignis* (Crocodyliformes: Mesoeucrocodylia) cranial anatomy and new data on the origin of the eusuchian-style palate. *Journal of Vertebrate Paleontology* 2008;**28**:382–408. https://doi.org/10.1671/0272-4634(2008)28[382:micmca]2.0.co;2

Turner AH, Pritchard AC. The monophyly of Susisuchidae (Crocodyliformes) and its phylogenetic placement in Neosuchia. *PeerJ* 2015;**3**:e759. https://doi.org/10.7717/peerj.759

Venczel M, Codrea VA. A new *Theriosuchus*-like crocodyliform from the Maastrichtian of Romania. *Cretaceous Research* 2019;**100**:24–38. https://doi.org/10.1016/j.cretres.2019.03.018

Vidal LM. Nota geologica y paleontologica sobre el Jurasico superior de la provincia de Lerida. *Boletin del Instituto Geologico de Espana* 1915;**16**:17–55.

Vogel S. Living in a physical world V. Maintaining temperature. *Journal of Biosciences* 2005;**30**:581–90. https://doi.org/10.1007/BF02703556

von Meyer H. Mittheilungen an Professor Bronn gerichtet. *Neues Jahrbuch für Mineralogie, Geognosie, Geologie und Petrefaktenkunde* 1850:195–204.

Vullo R, Néraudeau D. Cenomanian vertebrate assemblages from southwestern France: a new insight into the European mid-Cretaceous continental fauna. *Cretaceous Research* 2008;**29**:930–5. https://doi.org/10.1016/j.cretres.2008.05.010

Whetstone KN, Whybrow PJ. A cursorial crocodilian from the Triassic of Lesotho (Basutoland), southern Africa. *Occasional Papers of the Museum of Natural History, The University of Kansas* 1983;**106**:1–37.

Wilberg EW, Godoy PL, Griffiths EF *et al*. A new early diverging thalattosuchian (Crocodylomorpha) from the Early Jurassic (Pliensbachian) of Dorset, UK and implications for the origin and evolution of the group. *Journal of Vertebrate Paleontology* 2022:e2161909.

Winkler DA, Murry PA, Jacobs LL. Early Cretaceous (Comanchean) vertebrates of central Texas. *Journal of Vertebrate Paleontology* 1990;**10**:95–116. https://doi.org/10.1080/02724634.1990.10011794

Wu X-C, Sues H-D, Dong Z-M. *Sichuanosuchus shuhanensis*, a new ?Early Cretaceous protosuchian (Archosauria: Crocodyliformes) from Sichuan (China), and the monophyly of Protosuchia. *Journal of Vertebrate Paleontology* 1996a;**17**:89–103. https://doi.org/10.1080/02724634.1997.10010956

Wu X-C, Sues H-D, Brinkman DB. An atoposaurid neosuchian (Archosauria: Crocodyliformes) from the Lower Cretaceous of Inner Mongolia (People's Republic of China). *Canadian Journal of Earth Sciences* 1996b;**33**:599–605. https://doi.org/10.1139/e96-044

Wu X-C, Cheng Z-W, Russell AP. Cranial anatomy of a new crocodyliform (Archosauria: Crocodylomorpha) from the Lower Cretaceous of Song-Liao Plain, northeastern China. *Canadian Journal of Earth Sciences* 2001;**38**:1653–63. https://doi.org/10.1139/e01-055

Young C-C. Fossil crocodiles in China, with notes on dinosaurian remains associated with the Kansu crocodiles. *Bulletin of the Geological Society of China* 1948;**28**:255–88. https://doi.org/10.1111/j.1755-6724.1948.mp283-4011.x